uc 412

LBL-28845
Preprint

Lawrence Berkeley Laboratory
UNIVERSITY OF CALIFORNIA

Submitted to Astrophysical Journal

Structure and Stability of Rotating Relativistic Neutron Stars

F. Weber, N.K. Glendenning, and M.K. Weigel

May 1990

For Reference

Not to be taken from this room

LBL-28845
Copy 1
Bldg. 50 Library.

Prepared for the U.S. Department of Energy under Contract Number DE-AC03-76SF00098.

DISCLAIMER

This document was prepared as an account of work sponsored by the United States Government. While this document is believed to contain correct information, neither the United States Government nor any agency thereof, nor the Regents of the University of California, nor any of their employees, makes any warranty, express or implied, or assumes any legal responsibility for the accuracy, completeness, or usefulness of any information, apparatus, product, or process disclosed, or represents that its use would not infringe privately owned rights. Reference herein to any specific commercial product, process, or service by its trade name, trademark, manufacturer, or otherwise, does not necessarily constitute or imply its endorsement, recommendation, or favoring by the United States Government or any agency thereof, or the Regents of the University of California. The views and opinions of authors expressed herein do not necessarily state or reflect those of the United States Government or any agency thereof or the Regents of the University of California.

LBL - 28845

STRUCTURE AND STABILITY OF ROTATING RELATIVISTIC NEUTRON STARS*

F. Weber,† N. K. Glendenning, and M. K. Weigel‡

Nuclear Science Division
Lawrence Berkeley Laboratory
University of California
Berkeley, California 94720, U.S.A.

Subject headings: dense matter – equation of state – stars: neutron – stars: rotation

* This work was supported by the Director, Office of Energy Research, Office of High Energy and Nuclear Physics, Division of Nuclear Physics, of the U. S. Department of Energy under Contract DE-AC03-76SF00098 and by the Max-Kade Foundation of New York.

† Max Kade Foundation Research Fellow. Permanent address: Institute for Theoretical Physics, University of Munich, Theresienstrasse 37/III, D-8000 Munich 2, Federal Republic of Germany.

‡ Sektion Physik of the University of Munich, Am Coulombwall 1, D-8046 Garching, Federal Republic of Germany.

ABSTRACT

We investigate the influence of rotation on the bulk properties of neutron stars. Special emphasize is placed on the analysis of the maximum rotational frequency of the rotating star configurations. The calculations are based on different neutron matter equations of state. Two of them are calculated in the relativistic Hartree and Hartree-Fock approximation for electrically charge neutral many-baryon matter at zero temperature. The influence of two-particle correlations on the bulk properties of both rotating and non-rotating neutron stars is demonstrated through neutron matter equations of state calculated for the relativistic ladder approximation to the two-particle scattering matrix in matter by using the Holinde-Erkelenz-Alzetta (HEA) and Machleidt-Holinde-Elster (Bonn) meson-exchange potentials. We obtain from these two equations of state maximum rotating star models having Keplerian frequencies of $1.19 \cdot 10^3 \ \frac{1}{s}$ (HEA) and $9.8 \cdot 10^3 \ \frac{1}{s}$ $(Bonn)$ and gravitational masses of 2.51 and 2.25 $M_\odot$, respectively. From the study of the onset of instability modes caused by gravitational radiation and moderated by viscosity, performed for two rotating neutron star models with masses of 1.4 and 1.9 $M_\odot$, it follows that an $m = 4$ (or $m = 5$, favored by the larger mass model) instability is probably responsible for limiting the angular velocity of rotating neutron stars (and not the Keplerian frequency). The influence of viscosity on the limiting frequency is studied.

I. INTRODUCTION

Most of the neutron star calculations reported in the literature have been performed for non-rotating, spherically symmetric star configurations, whose properties are uniquely determined by the Oppenheimer-Volkoff equations (Oppenheimer and Volkoff 1939; Bowers, Gleeson, and Pedigo 1975*a*, *b*; Pandharipande, Pines, and Smith 1976; Arnett and Bowers 1977; Alonso and Ibanez Cabanell 1985; Glendenning 1985; Weber and Weigel 1989*a*). (Further references can be found in these publications.) However a steady increase in the number of observed rotating neutron stars with rotational periods in the millisecond range, e.g. (Shapiro and Teukolsky 1983, Backer and Kulkarni 1990) P(PSR 1937+21)=1.6 msec, P(PSR 1957+20)=1.6 msec, P(PSR 1913+16)=59.0 msec, has renewed considerable interest in the influence of rotation on the properties of such objects. Rotating neutron star calculations performed in the framework of Einstein's theory of general relativity are however relatively rare (Hartle and Thorne 1968; Baym, Pethick, and Sutherland 1971; Heintzmann, Hillebrandt, Eid, and Hilf 1974; Arnett and Bowers 1977; Datta and Ray 1983; Kapoor and Datta 1984; Ray and Datta 1984; Friedman, Ipser, and Parker 1986).

The basic input quantity encountered in the treatment of (rotating) neutron stars is the nuclear equation of state, i.e. the functional dependence of pressure on energy density $P = P(\epsilon)$, of neutron star matter. It is this quantity which connects nuclear and astrophysics with each other. The description of matter inside a star is a highly complicated many-body problem: Neutron stars are electrically charge neutral objects whose bulk amount of matter consists of a mixture of electrons, muons, and baryons. An elegant tool for treating the problem is the relativistic Green's function technique. Its systematic analysis leads in "lowest" order to the well-known Hartree and Hartree-Fock approximations. In the next step one arrives at the so-called Λ method which takes into account the influence of two-particle correlations in matter in terms of an effective scattering matrix. Neutron star

calculations within this framework have not been performed up to now.

A fundamental problem encountered in the treatment of rotating neutron stars is the question of stability of these objects. (1) The axisymmetric secular (i.e., dissipative) instability to differential rotation that would be excited by any operative viscosity. Once a rotating star configuration reaches the point at which this instability sets in, it would begin to rotate differentially and might then form a configuration consisting of a nearly uniformly rotating central bulge that continually transfers its angular momentum to a surrounding differentially rotating disk (Ostriker and Bodenheimer 1968, Durisen 1975). Other types of instabilities, however, are expected to grow on *shorter* time scales and may therefore appear before the above secular instability sets in. A dominant role in this context play the so-called (2) non-axisymmetric dynamical instabilities (Friedman and Schutz 1978, Friedman 1978). These are excited by gravitational radiation-reaction and moderated by viscosity (Lindblom 1986). An *absolute upper bound* on neutron star rotation finally is set by (3) the Keplerian angular velocity (Friedman, Ipser, and Parker 1986), defined by the balance of gravitational and centrifugal forces at the star's equator. Stars rotating at velocities larger than the Keplerian frequency become unstable because of mass shedding. We investigate in this article the onset of instabilities in rotating neutron stars which result from items (2) and (3).

First of all, we give a short description of the treatment of rotating neutron stars in the framework of general relativity in Section II. Different methods frequently used in the literature for determining the limiting frequency of a rotating star are discussed in greater detail. In Section III we discuss the equations of state (calculated for the relativistic Hartree, Hartree-Fock, and Λ approximation) used for our investigations. The results of our numerical investigation of the structure of rotating relativistic stars based on these equations of state are discussed in Section IV. There, the characteristics of the equations of state, which we believe incorporate the important physics of the nuclear many-body system, are discussed. The

stability problem of rotating neutron stars is investigated with respect to both the Keplerian limiting frequency as well as the onset of instabilities caused by non-axisymmetric secular modes. Our findings are summarized in Section V.

II. TREATMENT OF ROTATING NEUTRON STARS

One of the two major aspects of this article is concerned with the investigation of the properties of rotating neutron stars and the limiting rotational frequency a star can have before becoming unstable. The treatment of massive rotating stars in the framework of general relativity is a rather complicated task. Besides the numerical method of Butterworth and Ipser (Butterworth and Ipser 1976; Friedman, Ipser, and Parker 1986), developed so far for rotating fluid bodies of arbitrary frequency treated in general relativity, there exists the method of Hartle (Hartle 1967; Hartle and Thorne 1968) appropriate for stars which rotate at "small" angular velocities Ω (compared to the critical angular velocity Ω_c, see below). In the latter method (Hartle 1967) a perturbation solution based on the Schwarzschild metric

$$ds^2 = -e^{2\,\nu} dt^2 + e^{2\,\lambda} dr^2 + r^2 \left(d\theta^2 + \sin^2\theta \, d\phi^2\right) \tag{1.1}$$

is developed. Under the assumption that due to rotation the star distorts and effects the energy density and the pressure of the rotating fluid by amounts of $\Delta\epsilon$ and ΔP, respectively (i.e., the source term in the Einstein equation $G_{\mu\nu} = -8\pi\, G\, T_{\mu\nu}$ changes by $\Delta T_{\mu\nu}$), one can perform a multipole expansion of these quantities. In a similar fashion the metric is expanded through second order in the star's rotational frequency Ω (Ω is the angular velocity of the surface of the star relative to an observer at infinity (Hartle and Thorne 1968; Kapoor and Datta 1984)),

$$ds^2 = -e^{2\,\nu} dt^2 + e^{2\,\psi} \left(d\phi - \omega\, dt\right)^2 + e^{2\,\mu}\, d\theta^2 + e^{2\,\lambda} dr^2 + O\left(\frac{\Omega^3}{\Omega_c^3}\right), \tag{1.2}$$

where the metric functions are given by

$$e^{2\,\nu} = e^{2\,\Phi}[1 + 2\left(h_0 + h_2 P_2\right)], \tag{1.3}$$

$$e^{2\,\psi} = r^2 \sin^2\theta [1 + 2\left(v_2 - h_2\right) P_2], \tag{1.4}$$

$$e^{2\mu} = r^2[1 + 2\,(v_2 - h_2)\,P_2]\,, \tag{1.5}$$

$$e^{2\lambda} = \left(1 + \frac{2}{r}\,\frac{m_0 + m_2 P_2}{1 - \frac{2\,m\,G}{r}}\right)\,\left(1 - \frac{2\,m\,G}{r}\right)^{-1}\,. \tag{1.6}$$

$\Phi(r)$ in equation (1.3) denotes the gravitational potential and P_2 is the Legendre polynomial of order 2. $\omega(r)$ of equation (1.2) is the angular velocity of the local intertial frame and is proportional to Ω (dragging of local inertial frames). The perturbation functions m_0, m_2, h_0, h_2, v_2 are to be calculated from Einstein's field equations. Equation (1.2) is correct up to terms $O(\Omega^3/\Omega_c^3)$, where the critical velocity Ω_c is given by

$$\Omega_c \equiv \sqrt{M_s\,G/R_s^3} = 36\,\sqrt{[M_s/M_\odot]/[R_s/\mathrm{km}]^3}\,\cdot 10^4\,\frac{1}{\mathrm{s}}\,. \tag{1.7}$$

This corresponds to the Newtonian balance of centrifuge and gravity. Here, M_s and R_s denote the spherical star values of gravitational mass and radius, respectively. The Hartle method leads - in addition to the usual Oppenheimer-Volkoff equations which describe the corresponding spherically symmetric part of the rotating star - to additional sets of coupled monopole and quadrupole distribution functions. The full set of equations is rather lengthy and we refer the reader for more details to (Hartle 1967; Weber, Glendenning, and Weigel 1990).

In our investigation the assumption is made that the absolute upper limit on rotation is set by the Kepler frequency Ω_K, which is the maximum frequency a star can have before mass loss at the equator sets in (mass shedding). The expression for Ω_K, calculated in the frame of general relativity (denoted by Ω_K^{GR}), depends on the underlying metric (Friedman, Ipser, Parker 1986; Weber, Glendenning, and Weigel 1990),

$$\Omega_K^{GR} = e^{\nu-\psi}\;V\;+\;\omega, \qquad V \equiv \frac{\omega'}{2\psi'}\,e^{\psi-\nu}\,\sqrt{\frac{\nu'}{\psi'} + \left(\frac{\omega'}{2\psi'}\,e^{\psi-\nu}\right)^2}, \tag{1.8}$$

(c=1 in our units, all metric functions are to be evaluated at the equator, and primes denote derivatives with respect to the radial coordinate) and its value sets

an absolute upper limit on rotation because no uniformly rotating star can have $\Omega > \Omega_K$. We have calculated the expression for Ω_K^{GR} for the distorted Hartle metric of equations (1.2)-(1.6) in order to determine the limiting frequency. The resulting numerical outcome for Ω_K^{GR} can be compared with those values of Ω_K obtained in a different context. For example, the empirical expression (Friedman, Ipser, and Parker 1989),

$$\Omega_K^{FIP} \approx 24\sqrt{[M_s/M_\odot]/[R_s/\mathrm{km}]^3} \cdot 10^4 \frac{1}{\mathrm{s}} \qquad (\text{i.e.,} \quad \Omega_K^{FIP} \approx \frac{2}{3}\Omega_c)\,, \tag{1.9}$$

was established by an exact treatment of rapidly rotating fluid bodies in general relativity. (It should be noted that only the non-rotating (spherical) star properties enter in equation (1.9).) Ω_K^{FIP} of equation (1.9) is expected to be in agreement with Ω_K^{GR} of equation (1.8) by better than 10%. As pointed out by Friedman, Ipser, and Parker (1986), this estimate for the maximum rotational frequency is roughly consistent with the earlier prediction of Shapiro, Teukolsky, and Wasserman (1983) that the maximum frequency Ω_K for a given equation of state is proportional to $\sqrt{M_s/R_s^3}$. Ray and Datta (1984) exploit the onset of the nuclear instability of uniformly rotating, homogeneous Maclaurin Spheroids in order to obtain for the limiting frequency

$$\Omega_K^{RD} = 19\sqrt{[M_s/M_\odot]/[R_s/\mathrm{km}]^3} \cdot 10^4 \frac{1}{\mathrm{s}}\,, \tag{1.10}$$

a value which is slightly smaller than Ω_K^{FIP} of equation (1.9).

For later use we give the expressions for the frequency shifts of photons emitted at the equator in backward (B) and forward (F) direction, respectively (Friedman, Ipser, and Parker 1986),

$$z_{B\,/\,F} \quad = \quad \left(1 \pm \omega\, e^{\psi-\nu}\right)^{-1} \quad \left(\frac{1 \pm V}{1 \mp V}\right) \quad - \quad 1, \tag{1.11}$$

which is to be calculated at the star's equator. The polar redshift z_p is given by

$$z_p \quad = \quad e^{-\nu} \quad - \quad 1\,, \tag{1.12}$$

which is to be calculated at the star's pole.

III. THE NUCLEAR EQUATION OF STATE

a) General Aspects

Our second point of concern is the influence of the nuclear equation of state of infinite (electrically charge neutral) neutron star matter (Arnett and Bowers 1977; Glendenning 1985) - which serves as an input for solving the Oppenheimer-Volkoff or Hartle equations - on the bulk parameters of rotating neutron stars. A realistic determination of the equation of state has been the subject of much effort for many years without a general consensus (Glendenning 1988) on its behavior at higher densities, i.e. at $\varrho > \varrho_0$ ($\varrho_0 \approx 0.15\ \mathrm{fm}^{-3}$, density of normal nuclear matter). The models of neutron as well as nuclear matter treated so far differ mainly in the density dependence of the energy density, $\epsilon(\varrho)$. One can hope to shed light on the functional dependence of $\epsilon(\varrho)$ (Glendenning 1988) by applying different equations of state for solving stellar structure equations since knowledge of $\epsilon(\varrho)$ over a large density range (i.e., $\varrho < 10\,\varrho_0$) is necessary, and the bulk properties of the resulting star configuration are known to depend sensitively on the equation of state (Baym, Pethick, and Sutherland 1971; Bowers, Gleeson, and Pedigo 1975; Arnett and Bowers 1977; Glendenning 1985; Friedman, Ipser, and Parker 1986; Weber and Weigel 1989*a*).

The equations of state used in this work have been calculated for the relativistic Hartree (Glendenning 1985; Weber and Weigel 1989*a*) and Hartree-Fock (Weber and Weigel 1989*a*) approximation for charge neutral many-baryon/lepton neutron star matter. However, as a special feature here, we take the influence of two-particle correlations on the equation of state of neutron star matter into account, too. This goal can only be accomplished by going beyond the Hartree and Hartree-Fock treatments and requires the introduction of an effective interaction (two-particle potential, scattering (T) matrix) in neutron matter. We have calculated this interaction for neutrons in the medium in a self-consistent and co-

variant fashion (cf. below). The equations of state determined in this way can be classified as follows (for an overview, see Table 1):

(a) a relativistic Hartree equation of state (denoted by HV (Glendenning 1985; Weber and Weigel 1989*a*)) calculated for electrically charge neutral neutron star matter (at zero temperature) in generalized β equilibrium, allowing for the population of hyperon/baryon states with masses lower or equal to m_Δ,

(b) a relativistic Hartree-Fock equation of state (denoted by HFV (Weber and Weigel 1989)) calculated for matter under the same conditions as given in (a),

(c) a relativistic equation of state calculated for pure neutron matter at densities $0.02 < \varrho/\mathrm{fm}^{-3} < 0.28$ which takes into account $two - particle\ correlations$ (in the so-called Λ^{00} approximation (Wilets 1979, Poschenrieder and Weigel 1988*a*, *b*)) using the Machleidt-Holinde-Elster *Bonn* potential (Machleidt, Holinde, and Elster 1987) and is combined with the HV equation of state for $0.28 < \varrho/\ \mathrm{fm}^{-3} < 1.2$. The equation of state calculated in this way is denoted by $\Lambda^{00}_{Bonn} + HV$, and

(d) a relativistic equation of state similar to (c), but using the Holinde-Erkelenz-Alzetta (HEA) potential (Holinde, Erkelenz, and Alzetta 1972*a*, *b*).

For the neutron star calculations presented here, equations of state (a)-(d) have been combined with the ones of Harrison and Wheeler for the outer surface of the star, and Negele and Vautherin for the inner surface region (Glendenning 1985; Weber and Weigel 1989*a*).

b) Mathematical Framework

A consistent theoretical framework for deriving the equation of state on a level which allows the incorporation of two-particle correlations into the treatment of neutron and nuclear matter is the non-relativistic or relativistic Martin-Schwinger hierarchy of coupled Green's functions (Wilets 1979, Weigel and Wegmann 1971; Poschenrieder and Weigel 1988*a*, *b*). In the "lowest" order, the Martin-Schwinger

hierarchy can be truncated by factorizing the four-point Green's function into a (properly symmetrized) product of two-point Green's functions. This leads to the well-known Hartree (i.e. mean-field) and Hartree-Fock approximation. At this level of approximation, the Hartree-Fock treatment does not saturate nuclear matter for boson-exchange model potentials (Poschenrieder and Weigel 1988*b*). Therefore one must go beyond this.

The Λ (ladder) approximation scheme truncates the Martin-Schwinger hierarchy by factorizing the six-point Green's function into products of four- and two-point functions by which dynamical two-particle correlations in matter - which are connected with the two-body potential - are taken into account. The main problem which one encounters hereby is the calculation of the effective scattering matrix $< 12 \mid T^{ij} \mid 1'2' >$ in matter (Wilets 1979; Poschenrieder and Weigel 1988*a*, *b*), which is given by

$$T^{ij} = v - v^{ex} + \int v \, \Lambda^{ij} \, T^{ij} \, . \tag{3.1}$$

The basic input quantity in equation (3.1) is the nucleon-nucleon interaction in free space as derived, for example, in the Bonn meson-exchange model (Machleidt, Holinde, and Elster 1987). We have adopted the latest version of this interaction together with the HEA potential (Holinde, Erkelenz, and Alzetta 1972*a*, *b*) for the calculations presented here. A common feature of such models is that the potential parameters are adjusted to the two-body nucleon-nucleon scattering data, whereby - in this sense - a parameter-free treatment of the many-body problem is achieved.

The upper subscript on the T-matrix in equation (3.1) refers to different intermediate nucleon-nucleon propagators (Poschenrieder and Weigel 1988*a*, *b*). In the so-called Λ^{00} method, which has been applied for our calculations, both nucleons propagate freely in the intermediate particle states; the propagator Λ is thus given by a product of two free two-point Green's functions (denoted by g^0), $\Lambda^{00} = i g^0 \, g^0$. In the Λ^{10} treatment, which is presently under investigation, the

propagation of one nucleon in these states is coupled to the many-particle medium, g^1, while the other one propagates freely, i.e., $\Lambda^{10} = \frac{i}{2}(g^1\, g^0 + g^0\, g^1)$. (The Λ^{11} method, for which the motion of both nucleons is coupled to the medium, has been treated so far only for the non-relativistic approach (Weber and Weigel 1985).)

The Λ method has been shown to successfully describe the properties of normal nuclear matter at saturation density for both the non-relativistic (Weigel and Wegmann 1971; Weber and Weigel 1985) as well as relativistic case (Poschenrieder and Weigel 1988*a*, *b*). We would like to stress that the application of this method is certainly restricted to matter at not too high nuclear densities, i.e. $\varrho < (2-3)\,\varrho_0$. Otherwise correlations other than those taken into account in the Λ approach may become important (Weigel and Wegmann 1971; Wilets 1979). To mention several, these are many-body forces and modifications of the boson exchange description. Furthermore, the inclusion of hyperon degrees of freedom at larger densities in the Λ approach would require a knowledge of the hyperon-hyperon and hyperon-nucleon potentials to be used in conjunction with the Bonn and HEA potentials. A further problem concerns the non-renormalizability of the Λ method (Poschenrieder and Weigel 1988*a*, *b*). But in a first step one can render the theory finite by neglecting contributions arising from the negative-energy Dirac sea (no-sea approximation (Serot and Walecka 1986; Horowitz and Serot 1987)). In this respect the investigations performed by Glendenning (1989) are encouraging. There it has been shown that vacuum renormalization of relativistic nuclear field theory for both nuclear as well as neutron matter has negligible influence on the equation of state up to nuclear densities $\varrho \approx 10\varrho_0$, provided the coupling constants are tightly constrained by the five saturation properties of nuclear matter, i.e., binding energy, density, compression modulus, symmetry energy, and effective nucleon mass.

For this reasons we restrict ourselves to treating the Λ method (i.e., to taking into account the influence influence of two-particle correlations in the equation of state) only up to $\varrho < 1.7\,\varrho_0$. Beyond this density the population of hyper-

ons is expected to set in in charge neutral neutron star matter (Pandharipande 1971; Bowers, Gleeson, and Pedigo 1975*a*, *b*, Glendenning 1985; Weber and Weigel 1989*a*). We take this effect into account here by treating matter at $\varrho > 1.7\,\varrho_0$ in both the Hartree and Hartree-Fock approximation. This is supported by considering the high density behavior of the neutron (as well nuclear) matter equation of state calculated with and without two-particle correlations. As shown by Horowitz and Serot (1987), the Hartree, Hartree-Fock and relativistic Brueckner-Hartree-Fock equations of state approach each other for matter energy densities $\epsilon > 350$ MeV/fm^3 ($\varrho > 0.35$ fm^{-3}). (It is known (Poschenrieder and Weigel 1988*a*, *b*) that the relativistic Brueckner-Hartree-Fock approximation and the Λ method lead to similar results (see below).) This indicates that two-particle correlations influence the equation of state at most for densities $\varrho < 0.35$ fm^{-3}. Above this density a Hartree or Hartree-Fock treatment leads to essentially the same equation of state. The latter treatments however have the advantage, as already mentioned above, that the goal of incorporating additional hyperon/baryon degrees of freedom in combination with the occurrence of leptons can be achieved. In the low-density regime on the other hand, i.e. for $\varrho < \varrho_0/10$, the Hartree, Hartree-Fock and Λ equations of state tend towards each other since then medium effects become small: in terms of the particle's self-energy, Σ, which describes the influence of the medium on the nucleon propagation in matter, one has $\Sigma^\Lambda \simeq \Sigma^{HF} \ll m_N$ for $\varrho < \varrho_0/10$. Consequently a free-particle description takes over for such small nuclear densities which becomes the more accurate the lower the nuclear density ϱ is. The free-particle description is the low-density limit of the three treatments under consideration.

The above mentioned self-energy is defined in terms of the scattering matrix T in matter. The "Born" approximation of T sums the various meson potentials

of the nucleon-nucleon interaction in free space, i.e.,

$$< 12 \mid v \mid 1'2' >= \sum_{M=\sigma,\omega,\pi,\varrho,\eta,\delta,\phi} \delta^4_{11'}\ \delta^4_{22'}\ \Gamma^M_{11'}\ \Gamma^M_{22'}\ \Delta^M_{12}\ , \tag{3.2}$$

and leads to the well-known Hartree and Hartree-Fock approximation (Poschenrieder and Weigel 1988*a*, *b*; Weber and Weigel 1988; Weber and Weigel 1989*a*, *b*, *c*). The symbol Γ of equation (3.2) stands for the various meson-nucleon vertices (Holinde, Erkelenz, and Alzetta 1972*a*, *b*; Machleidt, Holinde, and Elster 1987), and Δ^M denotes the free meson propagator of a meson of type M.

The nucleon self-energy for these treatments can be represented schematically by (Poschenrieder and Weigel 1988*a*, *b*)

$$\Sigma^\Lambda = i \int [\, \mathrm{tr}\,(T\, g) - T\, g\,]\,, \qquad (\Lambda \text{ method}) \tag{3.3}$$

and (Weber and Weigel 1988; Weber and Weigel 1989*a*, *b*, *c*)

$$\Sigma^{B,\mathrm{HF}} = \sum_{M=\sigma,\omega\,\pi,\varrho} \sum_{B'=p,n,\Sigma^{\pm,0},\Lambda,\Xi^{0,-},\Delta^{++,+,0,-}} \int [\, \mathrm{tr}\,(\Delta^M\, g^{B'}) - \Delta^M\, g^{B'}\,]\,.$$

$$(\text{Hartree} - \text{Fock approximation}) \ \ldots\ldots\ldots\ldots\ldots\ldots\ldots\ldots\ldots\ldots \tag{3.4}$$

Equation (3.4) indicates that on the Hartree-Fock level the self-energies of the baryons of type B have been calculated by allowing for the population of all *charged* baryon states having masses lower or equal to the mass of the Δ-resonance. The nuclear forces in equation (3.4) are those of the scalar-vector-isovector model (cf. Table 1). The baryon propagators g^B in equations (3.3) and (3.4) satisfy Dyson's equation,

$$\left(\gamma^\mu\, p_\mu - m_B - \Sigma^B(p)\right)\, g^B(p) \ = \ -\,1 \tag{3.5}$$

which in turn terminates the set of equations that is to be solve self-consistently, subject to additional constraints like charge neutrality (Poschenrieder and Weigel

1988*a*, *b*; Weber and Weigel 1988; Weber and Weigel 1989*a*, *b*, *c*). As in the non-relativistic theory (Weigel and Wegmann 1971), it is sufficient for the calculations of the properties of the system to determine the so-called spectral function. One can deduce the following spectral representation for the Fourier transformed baryon propagator (Weber and Weigel 1989*a*):

$$g^B(p^\mu) = \int_{-\infty}^{+\infty} d\omega \, \frac{a^B(\omega, \vec{p})}{\omega - (p^0 - \mu^B)\,(1 + i\eta)} \, . \tag{3.6}$$

The rather complicated many-body problem is then shifted towards calculating the self-energies Σ^B in combination with the spectral functions a^B; the equation of state can be expressed solely in terms of these latter functions (Poschenrieder and Weigel 1988*a*, *b*; Weber and Weigel 1988; Weber and Weigel 1989*a*, *b*, *c*) and follows therefore immediately once self-consistent solutions of equations (3.1), (3.3), (3.5) in the case of the Λ method and (3.4), (3.5) for the Hartree-Fock treatment have been found.

IV. RESULTS AND DISCUSSION

a) Equation of State

In Table 2 the equations of state calculated for the Λ^{00} method using the Bonn and HEA potentials are listed. The nuclear densities range from 0.02 fm^{-3} up to 0.28 fm^{-3}. The values are graphically depicted in Figure 1. For the purpose of comparison we also show the HV and HFV equations of state (Weber and Weigel 1989*a*). According to the arguments given above, all equations of state tend toward each other for small values of the energy density ϵ (i.e. nuclear densities ϱ): $P^{\Lambda^{00}_{HEA}} \approx P^{\Lambda^{00}_{Bonn}} \approx P^{HV} \approx P^{HFV}(\epsilon)$ for ϵ <50 MeV/fm^3. As one can see, the HEA comes close to the HFV equation of state, and the $Bonn$ behaves parallel to the HV equation of state, with a constant pressure shift $P^{Bonn}(\epsilon) - P^{HV}(\epsilon) \approx$ 3 MeV/fm^3 for $\epsilon > 240$ MeV/fm^3. For $100 < \epsilon/\mathrm{MeV\,fm}^{-3} < 200$ both Λ equations of state show a significantly softer behavior than the HV and HFV which is caused by the inclusion of two-particle correlations within the former treatment. At larger values however the $Bonn$ equation of state becomes rather stiff. This behavior has also been found in the framework of relativistic Brueckner-Hartree-Fock calculations performed for the Bonn potential (Muether, Prakash, and Ainsworth 1987). This supports the observation that the relativistic Brueckner-Hartree-Fock and Λ approximation lead to similar results (Poschenrieder and Weigel 1988*a*, *b*). Furthermore from Figure 1 our motivation for combining the $Bonn$ and HV and the HEA and HFV equations of state with each other becomes clear.

In Figure 2 we display the different equations of state over a large ϵ range, $10 < \epsilon/\mathrm{MeV\,fm}^{-3} < 5{\cdot}10^3$, relevant for the treatment of neutron stars. (Typical values for the central energy density, ϵ_c, are $\sim 10^3$ MeV/fm^3.) One sees that the constraint of causality, $dP/d\epsilon < 1$, is fulfilled by our set of equations of state. It is known that the inclusion of the Fock (exchange) term - additionally to the Hartree (direct) term of the self-energy, stiffens the equation of state at larger densities

(Serot and Walecka 1986; Weber and Weigel 1988; Weber and Weigel 1989*a*, *b*, *c*). Because of the Fock term contained in HFV, the parameter set HFV gives more pressure for a given value of ϵ (> 500 MeV/fm^3) than the Hartree set HV. At high ϵ values $P^{HFV}(\epsilon)$ tends against $P^{HV}(\epsilon)$, which can be understood by analyzing the power dependence on density of the Hartree and Hartree-Fock equation of state (Serot and Walecka 1986). A special feature of the equations of state in use is the intersection of HFV and HV at $\epsilon_{cr} \approx 500$ MeV/fm^3. Above this value $P^{HFV}(\epsilon) > P^{HV}(\epsilon)$ according to the exchange term contained in the former treatment. We therefore call the HFV equation of state for this energy density range "stiffer" than the HV equation of state, and inversely the HFV "softer" than HV for ϵ values below ϵ_{cr}.

b) Keplerian Limiting Frequency

In this subsection we assume that the Keplerian frequency, defined by equation (1.8), sets the limit on stable neutron star rotation. By this, *absolute* upper limits on the parameters of these objects are set. The role of instability modes caused by gravitational radiation-reaction, which actually set the upper limit on rotation, will be discussed in the next subsection.

The dependence of the Keplerian angular velocity Ω_K on the gravitational neutron star mass is illustrated in Figure 3. These curves have been constructed in the framework of general relativity in the following way (Hartle and Munn 1975; Friedman, Ipser, and Parker 1986; Friedman, Ipser, and Sorkin 1988): (i) in the first step one starts with an arbitrarily chosen (small) value of the angular frequency $\tilde{\Omega}$ of the star (which remains fixed in the following) and calculates $\Omega_K^{GR}(\epsilon_c)$ for a variety of different central energy densities of the star. The solution of the Hartle equations (i.e., the perturbation functions mentioned in Section II) serves thereby as an input for calculating Ω_K^{GR} of equation (1.8). (ii) For a certain

value of ϵ_c, denoted by $\bar{\epsilon}_c$, one then finds $\Omega_K^{GR}(\bar{\epsilon}_c)=\tilde{\Omega}$ which is the star's maximum angular velocity for that value of ϵ_c as long as $[dM(\epsilon_c)/d\epsilon_c)]_{\bar{\epsilon}_c} > 0$ holds (i.e., as long as the gravitational mass of the *rotating* star $M(\epsilon_c)$ has not reached its maximum value). Otherwise the rotating star is unstable for this value of $\bar{\epsilon}_c$. This procedure is to be repeated for increasing values of $\tilde{\Omega}$ until a value of $\bar{\epsilon}_c$ is reached for which $[dM(\epsilon_c)/d\epsilon_c)]_{\bar{\epsilon}_c} < 0$. The (crossed) endpoint of each sequence shown in this Figure represents a star rotating at its absolute limiting frequency $\tilde{\Omega}^{\rm lim}$ which is defined by $\tilde{\Omega}^{\rm lim} \equiv \Omega_K^{GR}(\bar{\epsilon}_c^{\rm lim})$, $dM(\bar{\epsilon}_c^{\rm lim})/d\epsilon_c = 0$ and the condition that $dM(\bar{\epsilon}_c^{\rm lim})/d\epsilon_c < 0$ for values $\epsilon_c > \bar{\epsilon}_c^{\rm lim}$. The corresponding numerical results for $\tilde{\Omega}^{\rm lim}$ are given in the first row of Table 4. All the pulsars observed up to date (Backer and Kulkarni 1990) rotate at frequencies which are well below these values. (The claimed frequency $\Omega_{SN\,1987A} = 1.237 \cdot 10^4 \frac{1}{\rm s}$ has meanwhile been withdrawn.)

Figure 3 shows the dependence of the Keplerian frequency on the underlying equation of state. Different equations of state lead to quite different values for Ω_K^{GR} as a function of M (Friedman, Ipser, and Parker 1986). We illustrate this for both the HFV and HV equations of state (for the latter case the influence of two-particle correlations is shown too). The largest values for $\Omega_K^{GR}(M)$ result then from the asymptotically stiffest equation of state, HFV, followed by $\Omega_K^{GR,\Lambda^{00}_{Bonn}+HV}(M)$ and $\Omega_K^{GR,HV}(M)$. The reason for this behavior lies in the value of the star's radius: it is smaller for the Hartree-Fock equation of state (with and without two-particle correlations, cf. fifth row of Table 4); a smaller radius value however allows for a higher rotational frequency (in order to arrive at the same critical equatorial velocity (given by equation (1.8)) at which mass shedding sets in). The inclusion of two-particle correlations in the equation of state leads to smaller radius values too (cf. Table 4). These are taken into account in the combined $\Lambda^{00}_{Bonn} + HV$ equation of state. For that reason the values of $\Omega_K^{GR}(M)$ calculated for the $\Lambda^{00}_{Bonn} + HV$ equation of state lie above those calculated for HV, which neglects two-particle correlations.

It is interesting to note that our HFV and HV (and hence the Λ^{00}_{HEA} and $\Lambda^{00}_{Bonn} + HV$) equations of state exhibit the same qualitative pressure dependence $P(\epsilon)$ than equations of state labeled "B" (Pandharipande 1971, hyperonic model) and "D" (Bethe and Johnson 1974, model V), respectively, which have been used in the extensive neutron star studies performed by Arnett and Bowers (1977) and Friedman, Ipser, and Parker (1986). This can be seen from Figure 8, p. 38 in Bethe and Johnson (1974). The important point is that for energy densities $\epsilon < 1000$ MeV/fm^3, $P^B(\epsilon) < P^D(\epsilon)$ (which corresponds to $P^{HFV}(\epsilon) < P^{HV}(\epsilon)$ for $\epsilon < 500$ MeV/fm^3 in our case) and $P^B(\epsilon) > P^D(\epsilon)$ otherwise (in our case $P^{HFV}(\epsilon) > P^{HV}(\epsilon)$ for $\epsilon > 500$ MeV/fm^3). In other words, the equation of state "B" behaves asymptotically stiffer than "D" and inversely softer below the intersection (analogously to HFV and HV, respectively). Such a functional dependence of P on ϵ has an important impact on the Kepler frequency in so far that asymptotically stiffer equations of state ("B" and "HFV") lead to larger values for Ω^{GR}_K. Friedman, Ipser, and Parker (1989) find in their investigation for equation of state "B" significantly larger Kepler frequencies (as a function of spherical mass) than for "D". In agreement to this, the HFV equation of state leads to larger values for the Kepler frequencies in our investigation. This is in accord with the general finding (Glendenning 1989*b*) that for a neutron star to withstand fast rotation, the equation of state must be "soft" at low and intermediate densities, and "stiff" at high densities.

Table 3 contains the bulk properties calculated for the non-rotating neutron star models (Oppenheimer-Volkoff treatment). All values refer to stars at their maximum gravitational mass point. Our stiffest equation of state, HFV, leads to a slightly larger maximum stable mass (M^{HFV}=2.2 $M_\odot$) compared to HV (M^{HV} = 1.98 $M_\odot$). The incorporation of two-particle correlations is of minor influence on the maximum stable star mass for both Λ models under consideration. The calculated change in mass is smaller than 1%. The change in mass is however

the larger the smaller ϵ_c is: We find for star models with $\log[\epsilon_c/(\mathrm{g{\cdot}cm^{-3}})] < 14.65$ (i.e. ϵ_c <250 MeV/fm^3) a strong influence of these correlations on the mass of the star (Weber, Glendenning, and Weigel 1990). The change in radius (decrease) due to these correlations is found to be $\approx 4\%$. Thereby the fractional redshift z increases by $\approx 5\%$.

The bulk properties of neutron stars rotating at their maximum angular velocities Ω_K^{GR} are listed in Table 4. The first row gives the maximum Kepler velocities as calculated in this work in the framework of general relativity. The maximum masses calculated for the rotating star models are shown in the third row. They are largest for our asymptotically stiffest equation of state, i.e., $[M/M_\odot]_{HFV}$=2.52. The increase of mass due to rotation relative to the spherical mass value, $\Delta M/M_s$, is found to be of the order of 18% for the HFV model and 20% for the slightly softer HV model for rotation at the limiting frequency. We would like to stress that a mass increase of $\approx$ 20% can only be obtained if the construction of the rotating star model is performed self-consistently. Otherwise, i.e. when the maximum stable gravitational mass and radius of a $non-rotating$ star configuration are used in order to determine the limiting rotational frequency (cf. equations (1.7) and (1.10)), one obtains a mass increase of typically $\Delta M/M_s \approx 5\%$. For example, Datta and Ray (1983) find for the FP model (which can roughly be compared with our HFV model, see discussion below) for $\log[\epsilon_c/(\mathrm{g\cdot cm^{-3}})]$=15.48: Ω_K^{RD}=9480 $\frac{1}{\mathrm{s}}$, $\Delta M/M_s = 5.3\%$ and for $\log[\epsilon_c/(\mathrm{g\cdot cm^{-3}})]$=15.30: Ω_K^{RD}=8110 $\frac{1}{\mathrm{s}}$, $\Delta M/M_s = 6.3\%$. Friedman, Ipser, and Parker (1986) find for the same model - but solving Einstein's field equations exactly - for $\log[\epsilon_c/(\mathrm{g\cdot cm^{-3}})]$=15.40: $\Omega_K^{GR,FIP}$=12300 $\frac{1}{\mathrm{s}}$, $\Delta M/M_s = 17\%$. Our values are therefore of comparable size with those calculated by the latter authors. For all of their models they find an increase in mass ranging from 14 to 20 %, depending on the stiffness of the underlying equation of state. The increase of 18 to 20% found for our equations of state is in good agreement with those values and may give a hint that the Hartle formalism - de-

veloped for slowly rotating, massive objects - can be applied for the investigation of rotating star configurations with rotational frequencies of $\approx 10^4 \frac{1}{s}$, provided one treats the determination of the limiting frequency consistently. For the purpose of comparison we give in the fifth column of Table 4 (enclosed in round brackets) the Friedman, Ipser, and Parker (1986) outcome (exact treatment) of a maximum mass model calculation performed for the Friedman-Pandharipande equation of state (Friedman and Pandharipande 1981). The latter is denoted by FP. The reason for comparing the FP with HFV model lies in the similar quantitative behavior of $\Omega_K^{GR,FIP}(M)$ and $\Omega_K^{GR,HFV}(M)$ (Friedman, Ipser, and Parker 1989) and in the compatibility of the limiting angular velocities (cf. first row of Table 4). From this one may infer that the FP outcome can serve as a guideline. Indeed, most of the values of both of these columns are in good agreement and confirm the use of the Hartle method up to $\Omega \approx 10^4 \frac{1}{s}$ (for the deviations, see below).

c) Role of Secular Instability Modes

The values calculated for the ratio of rotational to gravitational energy, t (stability parameter), at the maximum mass star lie between 0.11 (HV) and 0.13 (HFV) for all parameter sets in use. For the purpose of comparison, Friedman, Ipser, and Parker (1986) find in their investigation t values in the range $0.09 < t < 0.133$ (the latter value refers to FP) for all sequences of equations of state studied there. Since the t value is proportional to the star's angular velocity Ω (cf. table caption 4), one can draw conclusions from this quantity about the star's instabilities against rotation.

As repeatedly stressed, we investigate in this work two different types of instabilities: the first one is that caused by rotation at the Keplerian frequency Ω_K^{GR} (beyond which mass shedding at the star's equator sets in); the second are related to instabilities driven by the growth of gravitational radiation secular instability modes (of the order m, which are moderated by viscosity ν) at certain critical

frequencies Ω_m^ν. From investigations of the gravitational radiation instabilities it is known that the $m = 3$ and $m = 4$ (Friedman 1983; Friedman, Ipser, and Parker 1986) or possibly the $m = 5$ (Lindblom 1986) instability modes (having angular behavior of the form $e^{i\,m\,\phi}$) set the limit on neutron star rotation. In the following we will show that for our equations of state these limiting frequencies Ω_m are in general *smaller* than the corresponding Keplerian velocities Ω_K^{GR}. This means in other words that the gravitational radiation instability sets the upper limit of neutron star rotation and *not* the Keplerian frequency.

According to Lindblom (1986), an estimate of the critical maximum angular velocity Ω_m can be obtained by solving

$$\Omega_m \;=\; \frac{\sigma_m(0)}{m}\left[\tilde{\alpha}_m(\Omega_m) + \tilde{\gamma}_m(\Omega_m)\left(\frac{\tau_{g,m}}{\tau_{\nu,m}}\right)^{\frac{1}{2\,m+1}}\right] \tag{4.1}$$

for these unknown frequencies. In this equation, $\sigma_m(0)$ are frequency functions, and $\tau_{g,m}$ and $\tau_{\nu,m}$ are the gravitational (growing) time scale of the mth instability mode, and the time scale that determines the rate at which this particlular mode is damped by virtue of viscosity, respectively (Lindblom 1986). The functions $\tilde{\alpha}_m$ and $\tilde{\gamma}_m$ contain information about the pulsation of the rotating star models and are difficult to determine. However, following the arguments of Lindblom (1986), it should be possible to obtain reasonably accurate estimates for Ω_m of equation (4.1) by replacing $\tilde{\alpha}$ and $\tilde{\gamma}$ by the Maclaurin spheroid functions, α_m and γ_m, respectively. Both of the latter functions do not depend strongly on the angular velocities Ω_m; one can therefore - in a reasonable first step - approximate them by $\alpha_m(\Omega_m) \equiv \gamma_m(\Omega_m) \approx \alpha_m(0) = \gamma_m(0) = 1$. The frequency functions, $\sigma_m(0)$, are given for the Maclaurin spheroids in the form (Lindblom 1986)

$$\sigma_m(0) \;=\; \Omega_c\,\sqrt{\frac{2\,m\,(m-1)}{2\,m\,+\,1}}\,, \tag{4.2}$$

with Ω_c defined by equation (1.7). The time scales in equation (4.1) for the growing of the gravitational radiation instability ($\tau_{g,m}$), which is moderated by viscosity

(after the growing time $\tau_{\nu,m}$), are given by the expressions

$$\tau_{g,m} = \frac{2}{3}\,\frac{(m-1)\,[(2m+1)!!]^2}{(m+1)\,(m+2)}\left(\frac{2m+1}{2m(m-1)}\right)^m \Omega_c^{-2(m+1)}\,R_s^{-(2m+1)}\,, \quad (4.3)$$

$$\tau_{\nu,m} = \frac{R_s^2}{(2m+1)\,(m-1)}\,\frac{1}{\nu}\,. \quad (4.4)$$

The quantity ν in equation (4.4) stands for the kinematic viscosity of neutron star matter for which we assume values in the range of $0 < \nu < 200\,\mathrm{cm}^2\,\mathrm{s}^{-1}$. For the purpose of orientation, a viscosity value of $\approx$ 100 cm^2 s^{-1} of neutron star matter corresponds to fluid temperatures of $T \approx 10^9$ K (Flowers and Itoh 1976; 1979). For decreasing temperatures, the viscosity increases rapidly like $\nu \propto T^{-2}$. A value of $\nu = 200$ cm^2 s^{-1} may serve as an rough upper bound on the viscosity of neutron star matter. Values of $\nu < 100$ cm^2 s^{-1} correspondingly refer to $T > 10^9$ K, which are expected to be reached in the interior of neutron stars in the first year after formation (Friedman 1983). Equations (4.1)-(4.4) have been treated for the relevant gravitational instability modes, i.e. m=3,4,5,6, and the case that ν lies in the above given interval. This will be discussed in the following.

The numerical outcome for the critical frequencies Ω_m, calculated for the instability modes m=3,4,5,6, is graphically depicted in Figure 4 for a neutron star whose gravitational mass is $M \approx 1.5\,M_\odot$. This mass value has been chosen in accordance with the mass of the binary pulsar PSR 1913+16 which has been accurately determined to be $(1.442 \pm 0.003)\ M_\odot$ (Taylor and Weisberg 1989). Typical rotational frequencies of (fast) pulsars lie in the millisecond range (cf. Section I). As an example, we pick out the frequency of the pulsar PSR 1937+21, $\Omega_{\rm fp} \equiv \Omega_{1937+21} = 4033\,\mathrm{s}^{-1}$ (Backer and Kulkarni 1990).

Figure 4 shows very clearly (1) the influence of the underlying equations of state (HV, $\Lambda^{00}_{Bonn} + HV$, HFV, and $\Lambda^{00}_{HEA} + HFV$, in this sequence from the bottom to the top of this figure), and (2) the influence of viscosity (ν=0, 1, 10, 100, and 200 cm^2 s^{-1}, from left to right) on the frequencies Ω_m at which the gravitational instability modes of order m set in. We find that for all four

equations of state Ω_m is smallest for $m = 4$ in the case of negligible viscosity (crossed endpoints to the left of the $m = 4$ lines in Figure 4). The case $\nu \approx 0$ corresponds to a newly formed (i.e., hot) neutron star, in which viscosity can be assumed to play only a minor role. The inverse situation is encountered in "old" (and therefore cold) neutron stars, which have relatively large (compared to young stars) viscosity values. However they can be spun up (and by this reheated) by accretion of mass from a companion. In this case the value of the viscosity is decreasing (from $\nu \approx 200$ cm^2 s^{-1} to $\nu \approx 0$ in our study). Figure 4 indicates that in the latter case the $m = 3$ mode possesses a lower frequency value Ω_m than the $m = 4$ mode. Since the minimum angular frequency Ω_m determines the *maximum angular velocity* of the stable Maclaurin spheroids, it follows from our approximative treatment of equation (4.1) that the limiting rotational frequency of a *young* rotating neutron star is determined by the $m = 4$ instability mode and that the $m = 3$ instability mode limits the increase of rotation of an *old* neutron star spun up by accretion. The computed limiting frequencies for the former case of a young neutron star ($\nu \approx 0$) are given in Table 5 and compared with the limiting *Keplerian* velocities Ω_K^{GR} for the different equations of state. It turns out that all frequencies $\Omega_{m=4}^{\nu=0}$ are roughly 40% smaller than the corresponding Keplerian values (cf. the curve in the right lower part of Figure 4). We would like to stress that due to our approximative method of determining Ω_m^ν, a more sophisticated treatment may lead to somewhat different values. However, the qualitative behavior of Ω_m^ν as functions of ν and m can be expected the remain unchanged.

The second largest frequencies are those of the $m = 5$ instability modes, followed by the ones of the $m = 3$ modes. This trend is consistent with the results computed by Lindblom (1986). He concludes that the $m = 4$ or $m = 5$ (rather than $m = 3$ or $m = 4$) instability is probably responsible for limiting the angular velocity of rotating neutron stars. (It should be noted that his investigation is based on a more sophisticated computation of the critical frequencies Ω_m (and of

course of different equations of state). For the purpose of comparison, we have also used his results of the fully general relativistic gravitational radiation time scales $\tau_{g,m}$ in order to determine Ω_m for our equations of state. It turned out that the deviations are largest for $m = 4$ and $m = 5$. To be more precisely, we obtained Ω_m values which are $\approx 16\%$ larger in the case of the $m = 4$ mode and $\approx 23\%$ larger for $m = 5$. However, the qualitative behavior of the different mode frequencies remained unchanged, i.e. the lower limit on rotation is set by the $m = 4$ mode, and all frequencies are smaller than Ω_K^{GR}.)

In summary, the various frequencies from above obey the inequalities $\Omega_{m=4}^{\nu=0} < \Omega_{m=3,5,6}^{\nu>0} < \Omega_K^{GR}$ for all of the equations of state of this work. The corresponding instability parameter values (t) mentioned at the beginning of this subsection have been calculated for the zero-viscosity $m = 4$ modes and are given, together with the Keplerian values, t_K, in Table 5. They satisfy the inequality relation $t_{m=4}^{\nu=0} < t_K$. A striking feature is that the t values of a star (of mass $M \approx 1.5\, M_\odot$) rotating at its Keplerian limiting frequency are significantly larger than those of a star rotating at a velocity at which the $m = 4$ mode instability sets in (frequency $\Omega_{m=4}^{\nu=0}$): in the former (Kepler) case one finds $t_K \approx 0.1$, whereas $t_{m=4}^{\nu=0} \approx 0.04$ in the latter situation. The difference in t comes obviously from the quite different rotational frequencies found in both of these cases. The frequencies Ω_m are however the larger the more massive the rotating star is. This is demonstrated for a rotating neutron star of mass $M = 1.9\ M_\odot$. Its instability frequencies, $\Omega_m^{\nu=0}$ as well as Ω_K^{GR}, are given by the numbers enclosed in round brackets in Table 5. A striking feature in this case is that $\Omega_{m=4}^{\nu=0} \approx \Omega_{m=5}^{\nu=0}$, whereas for the less massive star model ($M = 1.5\, M_\odot$) the frequency $\Omega_{m=4}^{\nu=0}$ clearly sets the lower bound on $\Omega_m^{\nu=0}$.

The *maximum* mass star model is obtained for rotation at the *maximum* Keplerian frequency (the outcome is listed in Table 4). Due to the changes of mass and radius, one finds $\Omega_{m=4}^{\nu=0} \to \Omega_K$ and $t_{m=4}^{\nu=0} \to t_K$. Only in this case the Keplerian frequency can be expected (if at all) to play a role by setting the upper

limit on stable neutron star rotation. Illustrated by means of Figure 4, this means that all left lying frequency curves Ω_m^ν will be shifted to the right (toward larger frequencies) until finally the $\Omega_{m=4}^{\nu=0}$ mode (setting the limit on rotation of young neutron stars) reaches the magnitude, or lies beyond, the corresponding Ω_K value.

The observed rotational frequency of the fast pulsar 1937+21, $\Omega_{\rm fp} = 4033\,{\rm s}^{-1}$, is also shown in Figure 4. It follows that our HV equation of state predicts a value for $\Omega_{m=4}^{\nu=0}$ (=3600 s^{-1}) that lies below $\Omega_{\rm fp}$. Therefore, this equation of state may be inappropriate for the description of this pulsar, provided that a more accurate treatment of equation (4.1) would lead to a similar quantitative result for $\Omega_{m=4}^{\nu=0}$. The three remaining equations of state give frequencies for the $m = 4$ mode at zero viscosity which are compatible with the existence of this pulsar (and the assumption that $M_{\rm fp} = 1.5\ M_\odot$). An interesting aspect related to this is concerned with the stiffness of the equation of state. The inclusion of two-particle correlations in neutron star matter in the HV equation of state shifts the value of $\Omega_{m=4}^{\nu=0}$ from 3600 s^{-1} to approximately 4000 s^{-1} (see second and third columns of Table 5). Therefore, in other words, equations (4.1)-(4.4) determining the onset of gravitational radiation instabilities, favor a rather soft behavior of the equation of state at not too large nuclear densities (which is the case for the Λ equation of state) accompanied by a significantly stiffer behavior otherwise (which is achieved by the Hartree (HV model) and Hartree-Fock (HFV model) treatments of high-density neutron star matter at large densities). This can be viewed of as an additional (independent) source supporting once again the general finding of Glendenning (1989*b*) mentioned in the foregoing subsection.

d) Further Quantities of Rotating Neutron Stars

Entries 11 to 15 of Table 4 are the injection energy (β), the velocity of a co-moving observer at the equator relative to a locally non-rotating observer (V of equation (1.8)), the values of equatorial redshift in backward (z_B) and forward

(z_F) direction of equation (1.11), and the polar redshift (z_p) of equation (1.12), respectively. These quantities have in common that they depend sensitively on the quantities of the deformed star (this concerns in particular the gravitational potential $\Phi(r)$ which is to be calculated at the star's equator and pole). For this reason, the FP values listed for V, z_B, z_F and z_p are to a less extent in agreement with ours. Friedman, Ipser, and Parker (1986) find for all models studied in their work $\mid z_B/z_F \mid \approx 6$, which is to be compared with $\mid z_B/z_F \mid \approx 4$ found here for our models. The large magnitude of this ratio reflects the considerable increase of the star's equatorial radius for rotation at the maximum Keplerian frequency.

Figure 5 displays the gravitational neutron star mass as a function of central energy density for both the non-rotating as well as rotating star models HV and $\Lambda^{00}_{Bonn}+HV$, respectively. The upper lying curves show the increase of mass due to rotation at the limiting frequency. Two-particle correlations soften the equation of state and hence lead in general to slightly smaller maximum stable masses. This can clearly be seen from Figure 5 (curves labeled HV and $\Lambda^{00}_{Bonn} + HV$). In the rotating case however their influence turns out to be much more drastic. For low values of ϵ_c (less gravitational attraction) the inclusion of two-particle correlations leads to star masses which are roughly 10% smaller than those found otherwise. The limiting frequencies remain nearly unchanged in this ϵ_c region, i.e., $\Omega_K^{GR,HV} \approx \Omega_K^{GR,\Lambda^{00}_{Bonn}+HV}$. For increasing values of ϵ_c ($\epsilon_c \rightarrow \epsilon_c^{\rm lim}$) the mass difference becomes smaller; but due to the fact that $R^{\Lambda^{00}_{Bonn}+HV} < R^{HV}$ (see Table 4) one finds for the Kepler frequency of both models at a given value of ϵ_c $\Omega_K^{GR,\Lambda^{00}_{Bonn}+HV} > \Omega_K^{GR,HV}$. In other words, stars of comparable gravitational mass have larger limiting frequencies if two-particle correlations in neutron star matter are taken into account. (Since the condensation of pions has the same quantitative influence on the neutron matter equation of state (Glendenning 1985), one may speculate that inclusion of this phenomenon changes the bulk properties of neutron stars in the same way. The same trend may also be obtained by the presence of

hyperons in neutron stars (Weber, Glendenning, and Weigel 1990).) Values of Ω_K^{GR} are drawn in in Figure 5 for a sample of different central energy densities.

Figures 6 and 7 show the curves of gravitational star mass as a function of equatorial radius. The underlying equations of state are HV, $\Lambda_{Bonn}^{00} + HV$ in Figure 6 and HFV, $\Lambda_{HEA}^{00} + HFV$ in Figure 7. It is known from Figure 5 that rotating stars of comparable mass rotate faster (and have larger values of ϵ_c) if the equation of state contains effects of two-particle correlations in matter. This is connected with a decrease of radius. The amount of decrease can be taken from Figures 6 and 7. The change is smaller for stars with larger ϵ_c values since then correlation effects are of less influence. The upper lying end points of each of these curves correspond to stars rotating at their limiting frequencies that are compatible with the equation of state in use.

The moment of inertia as a function of equatorial radius is displayed in Figure 8 for star models HV and $\Lambda_{Bonn}^{00} + HV$. The Λ model, characterized by smaller radii, leads correspondingly to smaller values for the moment of inertia. The effect is again less pronounced the larger the central energy density is.

Figure 9 illustrates the deformation of a star due to rotation at different limiting angular velocities. One finds a considerable deviation from spherical symmetry. The HV model predicts a rotating star with $\Omega_K^{GR,HV} = 9200\,\frac{1}{\mathrm{s}}$ for a central energy density $\epsilon_c = 1.43 \cdot 10^{15}$ g·cm^{-3}. As one can see, stars rotating at lower maximum frequencies have lower values of ϵ_c, e.g. for $\Omega_K^{GR,HV} = 6000\,\frac{1}{\mathrm{s}}$ one finds $\epsilon_c = 0.59 \cdot 10^{15}$ g·cm^{-3}. This is however connected with a simultaneous inflation of the star.

V. SUMMARY

In summary, we studied in this work the influence of two-particle correlations on the bulk properties of rotating and non-rotating neutron stars. The investigation is based on Hartle's formalism, developed originally for slowly rotating, massive objects in the frame of general relativity (but used by Hartle and Thorne (1968) for frequencies up to $\approx 2 \cdot 10^4 \frac{1}{s}$). We have demonstrated that when using a proper method for constructing the limiting rotational velocity of a neutron star, Hartle's formalism leads to results for the bulk properties of maximum rotating models that are of comparable size with those obtained by solving the more difficult Einstein field equations exactly. The maximum angular velocity predicted by our calculations are $9.2 \cdot 10^3 \frac{1}{s}$ for the relativistic Hartree equation of state HV and $1.18 \cdot 10^3 \frac{1}{s}$ for the relativistic Hartree-Fock equation of state.

Two-particle correlations influence the neutron matter equation of state at most for $\varrho \approx (1-2)\varrho_0$ (softening) and hence are of considerable influence on the properties of lighter neutron stars. As it turned out, inclusion of these correlations changes the properties of the maximum star models only slightly: one obtains a less massive star with a slightly smaller value of radius. By having a smaller radius, the star is allowed to rotate at a higher maximum angular velocity (cf. Table 4). For example, the Kepler frequencies are shifted thereby from the values quoted above to $9.8 \cdot 10^3 \frac{1}{s}$ (*Bonn* potential) and $1.19 \cdot 10^3 \frac{1}{s}$ (HEA). The stiffer behavior of the HFV equation of state counterbalances the influence of two-particle correlations on the star's radius.

The ratio $(t \equiv)\ T/\mid W \mid$ of rotational to gravitational energy is an important parameter which gives a hint concerning the onset of instability modes. Its values are found to lie in the range of $0.11 < T/\mid W \mid < 0.13$ for star models rotating at their respective *maximum Keplerian* frequencies (Table 4). From this it would follow that instability against a bar ($m = 2$) mode, which is expected to set in at $t_{m=2} \approx 0.14$, appears unlikely since $t_K < t_{m=2}$. However, as clearly shown

by our investigation, the limiting frequency of a rotating neutron star is *not* set by the Keplerian frequency Ω_K^{GR}, but by the $m = 4$ or more probably by the $m = 5$ instability modes (frequencies $\Omega_{m=4}^{\nu=0}$ and $\Omega_{m=5}^{\nu=0}$, respectively). The latter mode is favored by massive (i.e., $M \approx 1.9\, M_\odot$) rotating neutron stars. We have demonstrated this behavior by treating two rotating star models of gravitational masses 1.4 and 1.9 $M_\odot$ (cf. Table 5). The above results refer to zero-viscosity ($\nu = 0$) neutron stars and are therefore restricted to young objects. The influence of non-zero viscosity values on the frequencies Ω_m is investigated by treating viscosities in the range of $0 < \nu < 200$ cm^2 s^{-1}.

A further interesting quantity - which gives a hint about the amount of deformation due to rotation - is the ratio of backward to forward redshifts of photons emitted at the star's equator. We find a value of ≈ 4. The large magnitude reflects the large increase in radius for stars rotating at the absolute maximum frequency $\Omega \approx \Omega_K^{GR}$.

Acknowledgment

One of us (F. W.) thanks the President of the Max Kade Foundation of New York for a grant.

This work was supported by the Director, Office of Energy Research, Office of High Energy and Nuclear Physics, Division of Nuclear Physics, of the U. S. Department of Energy under Contract DE-AC03-76SF00098 and by the Max Kade Foundation of New York.

Table 1

EQUATIONS OF STATE OF THIS WORK

Model	Equation of state (Interactions)	Mass density range † [g/cm^3]	Composition
	Harrison-Wheeler	$7.8 < \epsilon < 10^{11}$	Crystalline; light metals, electron gas
	Negele-Vautherin	$10^{11} < \epsilon < 10^{13}$	Crystalline; heavy metals, relativistic electron gas
Λ^{00}_{Bonn}	Relativistic Λ^{00} approximation (T matrix); based on the Bonn meson-exchange potential $(\sigma, \omega, \pi, \varrho, \eta, \delta)$	$10^{13} < \epsilon < 5 \cdot 10^{14}$	Neutrons
Λ^{00}_{HEA}	Same; based on the HEA meson-exchange potential $(\sigma, \omega, \pi, \varrho, \eta, \delta, \phi)$	$10^{13} < \epsilon < 5 \cdot 10^{14}$	Neutrons
HV	Relativistic Hartree approximation $(\sigma, \omega, \varrho)$‡	$10^{13} < \epsilon < 9 \cdot 10^{15}$	p, n, Λ, $\Sigma^{\pm,0}$, $\Xi^{0,-}$; e^-, μ^-
HFV	Relativistic Hartree-Fock approximation $(\sigma, \omega, \pi, \varrho)$	$10^{13} < \epsilon < 9 \cdot 10^{15}$	p, n, Λ, $\Sigma^{\pm,0}$, $\Xi^{0,-}$, Δ^-; e^-, μ^-

†) The conversion of ϵ from MeV/fm^3 to g/cm^3 can be accomplished by multiplying the former quantity with $1.783 \cdot 10^{12}$.

‡ "V" takes reference to the notation introduced in earlier works (Weber and Weigel 1989*a*, *b*).

Table 2

Λ^{00} NEUTRON MATTER EQUATIONS OF STATE CALCULATED USING THE BONN AND HEA MESON-EXCHANGE POTENTIALS

Bonn potential			HEA potential		
ϱ [fm^{-3}]	ϵ [MeV fm^{-3}]	P [MeV fm^{-3}]	ϱ [fm^{-3}]	ϵ [MeV fm^{-3}]	P [MeV fm^{-3}]
0.02126	20.00	0.0334	0.02127	20.00	0.0339
0.03187	30.00	0.0716	0.03187	30.00	0.0729
0.04246	40.00	0.1252	0.04247	40.00	0.1256
0.05304	50.00	0.1940	0.05304	50.00	0.1928
0.06360	60.00	0.2543	0.06360	60.00	0.2571
0.07415	70.00	0.2881	0.07415	70.00	0.3038
0.08470	80.00	0.3168	0.08470	80.00	0.3422
0.09524	90.00	0.3726	0.09524	90.00	0.3889
0.10577	100.00	0.4867	0.10577	100.00	0.4722
0.11629	110.00	0.6732	0.11629	110.00	0.6267
0.12678	120.00	0.9309	0.12679	120.00	0.8547
0.13725	130.00	1.2422	0.13727	130.00	1.1177
0.14770	140.00	1.5604	0.14773	140.00	1.3756
0.15812	150.00	1.8597	0.15817	150.00	1.6159
0.16853	160.00	2.2221	0.16860	160.00	1.9403
0.17890	170.00	2.7560	0.17899	170.00	2.5268
0.18923	180.00	3.5382	0.18934	180.00	3.5641
0.19951	190.00	4.6249	0.19961	190.00	5.0433
0.20973	200.00	6.0850	0.20981	200.00	6.7660
0.21987	210.00	8.0066	0.21991	210.00	8.5651
0.22990	220.00	10.4791	0.22993	220.00	10.3642
0.23981	230.00	13.5411	0.23987	230.00	12.1043
0.24956	240.00	16.8402	0.24973	240.00	13.7560

0.25920	250.00	19.8478	0.25953	250.00	15.3049
0.26876	260.00	22.3301	0.26928	260.00	16.7614
0.27827	270.00	24.5069	0.27902	270.00	18.1674

Table 3

BULK PROPERTIES OF NON-ROTATING NEUTRON STARS CALCULATED FOR THE MAXIMUM STABLE GRAVITATIONAL MASS†

	HV	$\Lambda^{00}_{Bonn} + HV$	HFV	$\Lambda^{00}_{HEA} + HFV$
$\log[\epsilon_c/(\mathrm{g} \cdot \mathrm{cm}^{-3})]$	15.37	15.37	15.38	15.38
$M/M_\odot$	1.976	1.969	2.198	2.195
R [km]	11.34	10.97	10.70	10.63
$\log[I/(\mathrm{g} \cdot \mathrm{cm}^2)]$	45.31	45.30	45.38	45.38
z	0.4355	0.4593	0.5945	0.6018

†) I and z denote the moment of inertia and the fractional redshift, respectivley. All other entries are explained in the text.

Table 4

INFLUENCE OF ROTATION ON THE PROPERTIES OF NEUTRON STARS

	HV	$\Lambda^{00}_{Bonn} + HV$	HFV (FP)	$\Lambda^{00}_{HEA} + HFV$
Ω_K^{GR} $[10^4\ \frac{1}{s}]$	0.92	0.98	1.18 (1.23)	1.19
$\log[\epsilon_c/(\mathrm{g}\cdot\mathrm{cm}^{-3})]$	15.15	15.15	15.23 (15.40)	15.23
$M/M_\odot$	2.26	2.25	2.52 (2.30)	2.51
$\Delta M/M_s$ †	0.20	0.20	0.18 (0.17)	0.18
R_{eq} [km] ‡	14.8	14.2	13.0 (12.0)	12.9
R_p [km]	10.2	9.6	9.0	8.9
R_{eq}/R_s	1.18	1.18	1.15	1.15
R_p/R_s	0.81	0.80	0.80	0.79
$\log[I/(\mathrm{g}\cdot\mathrm{cm}^2)]$	45.36	45.35	45.39 (45.38)	45.39
t *	0.11	0.12	0.13 (0.13)	0.13
β	0.31	0.28	0.15 (0.28)	0.14
V_{eq}	0.55	0.56	0.64 (0.49)	0.64
z_B	2.23	2.31	2.99 (2.63)	3.02
z_F	-0.69	-0.70	-0.74 (-0.32)	-0.75
z_p	0.79	0.90	1.59 (1.89)	1.64
e	0.73	0.74	0.73 (0.67)	0.73
$\Pi/(M_s R_s^2)$	0.052	0.059	0.048	0.049

†) The lower subscript s on M and R denotes the values of the corresponding non-rotating, spherical star model. ΔM stands for the increase of (gravitational) mass due to rotation.

‡) eq and p refer to equator and pole, respectively.

*) The stability parameter t is defined by (Friedman, Ipser, and Parker 1986) $t \equiv T/\mid W \mid$, $T \equiv \frac{J\Omega}{2}$, $W = M_{proper} + T - M$; β is the injection energy: $\beta \equiv e^{2\nu}\mid_{pole} = \frac{1}{(z_p+1)^2}$. The eccentricity e is given by $e = \sqrt{1-(R_p/R_{eq})^2}$. Π stands for the quadrupole moment (Hartle 1968).

Table 5

ONSET OF THE $m = 3, 4, 5, 6$ INSTABILITY MODES IN ROTATING NEUTRON STARS OF MASSES $M = 1.5\,M_\odot$ and $M = 1.9\,M_\odot$

	HV	$\Lambda^{00}_{Bonn} + HV$	HFV	$\Lambda^{00}_{HEA} + HFV$
$\Omega^{\nu=0}_{m=3}$ $[\frac{1}{s}]$ *	3700	4150	4500	4650
	(4960)	(5450)	(5500)	(5600)
$\Omega^{\nu=0}_{m=4}$ $[\frac{1}{s}]$	3600	4000	4400	4500
	(4800)	(5280)	(5340)	(5430)
$\Omega^{\nu=0}_{m=5}$ $[\frac{1}{s}]$	3650	4070	4450	4580
	(4890)	(5270)	(5330)	(5420)
$\Omega^{\nu=0}_{m=6}$ $[\frac{1}{s}]$	3870	4300	4660	4800
	(4970)	(5440)	(5490)	(7180)
$t^{\nu=0}_{m=4}$ †	0.035	0.038	0.037	0.038
$t^{\nu=0}_{m=5}$	(0.042)	(0.045)	(0.041)	(0.041)
Ω^{GR}_{K} $[\frac{1}{s}]$ ‡	5600	6950	6900	7300
	(7300)	(8200)	(8480)	(8700)
t_K †, ‡	0.096	0.107	0.105	0.107
	(0.104)	(0.114)	(0.115)	(0.117)

* Given are the critical zero-viscosity ($\nu = 0$) angular velocities. The values enclosed in round brackets refer to the $M = 1.9\,M_\odot$ star model, the values above them to $M = 1.5\,M_\odot$. The $m = 4$ frequencies determine the lower bound on Ω_m for the less massive star and therefore set the limit on rotation of a newly formed (i.e., hot) neutron star of this mass. For $M = 1.9\,M_\odot$,

however, the $m = 5$ frequencies are close to (or even lie below) the $m = 4$ values.

†) The quantities $t_{m=4}^{\nu=0}$ and t_K denote the stability parameter t (defined in Table 4) that corresponds to the $\Omega_{m=4}^{\nu=0}$ mode, and the Keplerian angular velocity Ω_K^{GR}, respectively.

‡ These values are taken from Weber, Glendenning, and Weigel (1990).

References

Alonso, J. D., and Ibanez Cabanell, J. H. 1985, *Ap. J.*, **291**, 308.

Arnett, W. D., and Bowers, R. L. 1977, *Ap. J.*, **33**, 415, and references contained therein.

Backer, D. C., and Kulkarni, S. R. 1990, *Phys. Today*, **43**, 26.

Baym, G., Pethick, C., and Sutherland, P. 1971, *Ap. J.*, **170**, 299.

Bethe, H. A., and Johnson, M. B. 1974, *Nucl. Phys.*, **A230**, 1.

Bowers, R. L., Gleeson, A. M., and Pedigo, R. D. 1975*a*, *Phys. Rev.*, **D12**, 3043.

Bowers, R. L., Gleeson, A. M., and Pedigo, R. D. 1975*b*, *Phys. Rev.*, **D12**, 3056.

Butterworth, E. M., and Ipser, J. R. 1976, *Ap. J.*, **204**, 200.

Datta, B., and Ray, A. 1983, *Mon. Not. R. astr. Soc.*, **204**, 75P.

Durisen, R. H. 1975, *Ap. J.*, **199**, 179.

Flowers, E., and Itoh, N. 1976, *Ap. J.*, **206**, 218.

Flowers, E., and Itoh, N. 1979, *Ap. J.*, **230**, 847.

Friedman, J. L. 1978, *Comm. Math. Phys.*, **62**, 247.

Friedman, J. L. 1983, *Phys. Rev. Lett*, **51**, 11.

Friedman, J. L., Ipser, J. R., and Parker, L. 1986, *Ap. J.*, **304**, 115.

Friedman, J. L., Ipser, J. R., and Parker, L. 1989, *Phys. Rev. Lett.*, **62**, 3015.

Friedman, J. L., Ipser, J. R., and Sorkin, R. D. 1988, *Ap. J.*, **325**, 722.

Friedman, B., Pandharipande, V. R. 1981, *Nucl. Phys.*, **A361**, 502.

Friedman, J. L., and Schutz, B. F. 1978, *Ap. J.*, **222**, 281.

Glendenning, N. K. 1985, *Ap. J.*, **293**, 470, and references contained therein.

Glendenning, N. K. 1988, *Phys. Rev.*, **C37**, 2733, and references contained therein.

Glendenning, N. K. 1989, *Nucl. Phys.*, **A493**, 521.

Hartle, J. B. 1967, *Ap. J.*, **150**, 1005.

Hartle, J. B., and Munn, M. W. 1975, *Ap. J.*, **198**, 467.

Hartle, J. B., and Thorne, K. S. 1968, *Ap. J.*, **153**, 807.

Heintzmann, H., Hillebrandt, W., Eid, M. F., and Hilf, E. R. 1974, *Z. Naturforsch.*, **29a**, 933.

Holinde, K., Erkelenz, K., and Alzetta, R. 1972*a*, *Nucl. Phys.*, **A194**, 161.

Holinde, K., Erkelenz, K., and Alzetta, R. 1972*b*, *Nucl. Phys.*, **A198**, 598.

Horowitz, C. J., and Serot, B. D. 1987, *Nucl. Phys.*, **A464**, 613.

Kapoor, R. C., and Datta, B. 1984, *Mon. Not. R. astr. Soc.*, **209**, 895.

Lindblom, L. 1986, *Ap. J*, **303**, 146.

Machleidt, R., Holinde, K., and Elster, Ch. 1987, *Phys. Rep.*, **149**, 1.

Muether, H., Prakash, M., and Ainsworth, T. L. 1987, *Phys. Rev. Lett.*, **199B**, 469.

Oppenheimer, J. R., and Volkoff, G. M. 1939, *Phys. Rev.*, **55**, 374.

Ostriker, J. P., and Bodenheimer, P. 1968, *Ap. J.*, **151**, 1089.

Pandharipande, V. R. 1971, *Nucl. Phys.*, **A178**, 123.

Pandharipande, V. R., Pines, D., Smith, R. A. 1976, *Ap. J.*, **208**, 550.

Poschenrieder, P., and Weigel, M. K. 1988*a*, *Phys. Lett.*, **B200**, 231.

Poschenrieder, P., and Weigel, M. K. 1988*b*, *Phys. Rev.*, **C38**, 471.

Ray, A., and Datta, B. 1984, *Ap. J.*, **282**, 542.

Serot, B. D., and Walecka, J. D. 1986, *Adv. Nucl. Phys.*, **16**, 1.

Shapiro, S. L., and Teukolsky, S. A. 1983, *Black holes, white dwarfs and neutron stars* (New York: McGraw-Hill).

Shapiro, S. L., Teukolsky, S. A., and Wasserman, I. 1983, *Ap. J.*, **272**, 702.

Taylor, J. H., and Weisberg, J. M. 1989, *Ap. J.*, **345**, 434.

Weber, F., Glendenning, N. K., and Weigel, M. K. 1990, *Rotating Relativistic Neutron Stars* (LBL preprint).

Weber, F., and Weigel, M. K. 1985, *Phys. Rev.*, **C32**, 2141.

Weber, F., and Weigel, M. K. 1988, *Z. Phys.*, **A330**, 249.

Weber, F., and Weigel, M. K. 1989*a*, *Nucl. Phys.*, **A505**, 779, and references contained therein.

Weber, F., and Weigel, M. K. 1989*b*, *Nucl. Phys.*, **A493**, 549.

Weber, F., and Weigel, M. K. 1989*c*, *J. Phys.*, **G15**, 765.

Weigel, M. K., and Wegmann, G. 1971, *Fortschr. Phys.*, **19**, 451.

Wilets, L. 1979, *Green's functions method for the relativistic field theory many – body problem*, *in Mesons in nuclei*, *vol. III* (Amsterdam: North-Holland), p. 737.

Figure Captions

Fig. 1. Neutron matter equations of state, pressure vs. energy density, calculated for the relativistic Λ method using the Bonn and HEA potentials. HV and HFV refer to equations of state calculated for the relativistic Hartree and Hartree-Fock approximation to electrically charge neutral many-baryon/lepton matter.

Fig. 2. Sequence of equations of state used in this work shown over a wide range of energy densities relevant for neutron star calculations. The symbols ϵ_0, ϵ_{HFV}, and ϵ_{HV} denote the energy density of normal nuclear matter and the values at which the population of hyperons for the HFV and HV equations of state sets in, respectively.

Fig. 3. Kepler angular velocity Ω_K^{GR} vs. gravitational mass of a rotating neutron star for different equations of state. The end points of each sequence marked by a cross correspond to the maximum Kepler frequencies.

Fig. 4. Critical angular velocities Ω_m^ν and Ω_K^{GR} at which instability against gravitational radiation-reaction and mass shedding (lowest horizontal line) at the star's equator sets in, respectively, calculated for a rotating star model of gravitational mass $M = 1.5\,M_\odot$ (the values are listed in Table 5). The frequencies Ω_m^ν are shown for instability modes $m = 3, 4, 5, 6$ for the four equations of state of this work, i.e., HV, $\Lambda_{Bonn}^{00} + HV$, HFV, and $\Lambda_{HEA}^{00} + HFV$ (from the bottom to the top). The left lying crosses denote the *maximum* rotational frequencies, which are set by the (small viscosity, $\nu \approx 0$) $\Omega_{m=3}^{\nu=0}$ modes calculated from these equations of state. The tick marks refer to viscosities ν =1,10,100, and 200 cm^2 s^{-1} (in this order from left to right). These frequencies are to be compared with the corresponding Keplerian values, which are given for the four equations of state by the crossed points shown at the bottom of this figure. The straight vertical line denotes the frequency of PSR 1937+21: $\Omega_{\rm fp} = 4033$ s^{-1}.

Fig. 5. Gravitational star mass vs. central energy density for star models HV and $\Lambda^{00}_{Bonn}+HV$. The upper lying curves refer to stars rotating at their maximum Kepler velocities (the numbers attached to this curves refer to the Ω^{GR}_K), the lower curves belong to non-rotating star models.

Fig. 6. Gravitational mass vs. equatorial radius calculated for stars rotating at their maximum angular velocity Ω^{GR}_K (number in round brackets). The underlying models are HV and $\Lambda^{00}_{Bonn}+HV$. Along each curve, crosses are labeled with the values of the model's central energy density in units of 10^{15} g·cm^{-3}.

Fig. 7. Gravitational mass vs. equatorial radius as in Figure 5, but calculated for models HFV and $\Lambda^{00}_{HEA}+HFV$.

Fig. 8. Moment of inertia vs. equatorial radius calculated for stars at their maximum angular velocity Ω^{GR}_K (numbers in round brackets). The underlying models are HV and $\Lambda^{00}_{Bonn}+HV$. Along each curve, crosses are labeled with the values of the model's central energy density in units of 10^{15}g· cm^{-3}.

Fig. 9. Rotational deformation for different maximum angular frequencies Ω^{GR}_K (numbers in round brackets). The origin of the coordinate axis is viewed of as being fixed at the star's center. The vertical axis points to the star's pole, the horizontal axis to its equator. The numbers attached to each of these curves refer to the value of the corresponding central energy density ϵ_c in units of 10^{15} g·cm^{-3}.

Postal Addresses

Norman K. Glendenning, Lawrence Berkeley Laboratory, Nuclear Science Division, University of California, 1 Cyclotron Road, Berkeley, California 94720, U.S.A.

Fridolin Weber, Lawrence Berkeley Laboratory, Nuclear Science Division, University of California, 1 Cyclotron Road, Berkeley, California 94720, U.S.A.; permanent address: Institute for Theoretical Physics, Ludwig-Maximilians University of Munich, Theresienstrasse 37/III, D-8000 Munich 2, F.R.G.

Manfred K. Weigel, Sektion Physik of the Ludwig-Maximilians University of Munich, Am Coulombwall 1, D-8046 Garching, F.R.G.

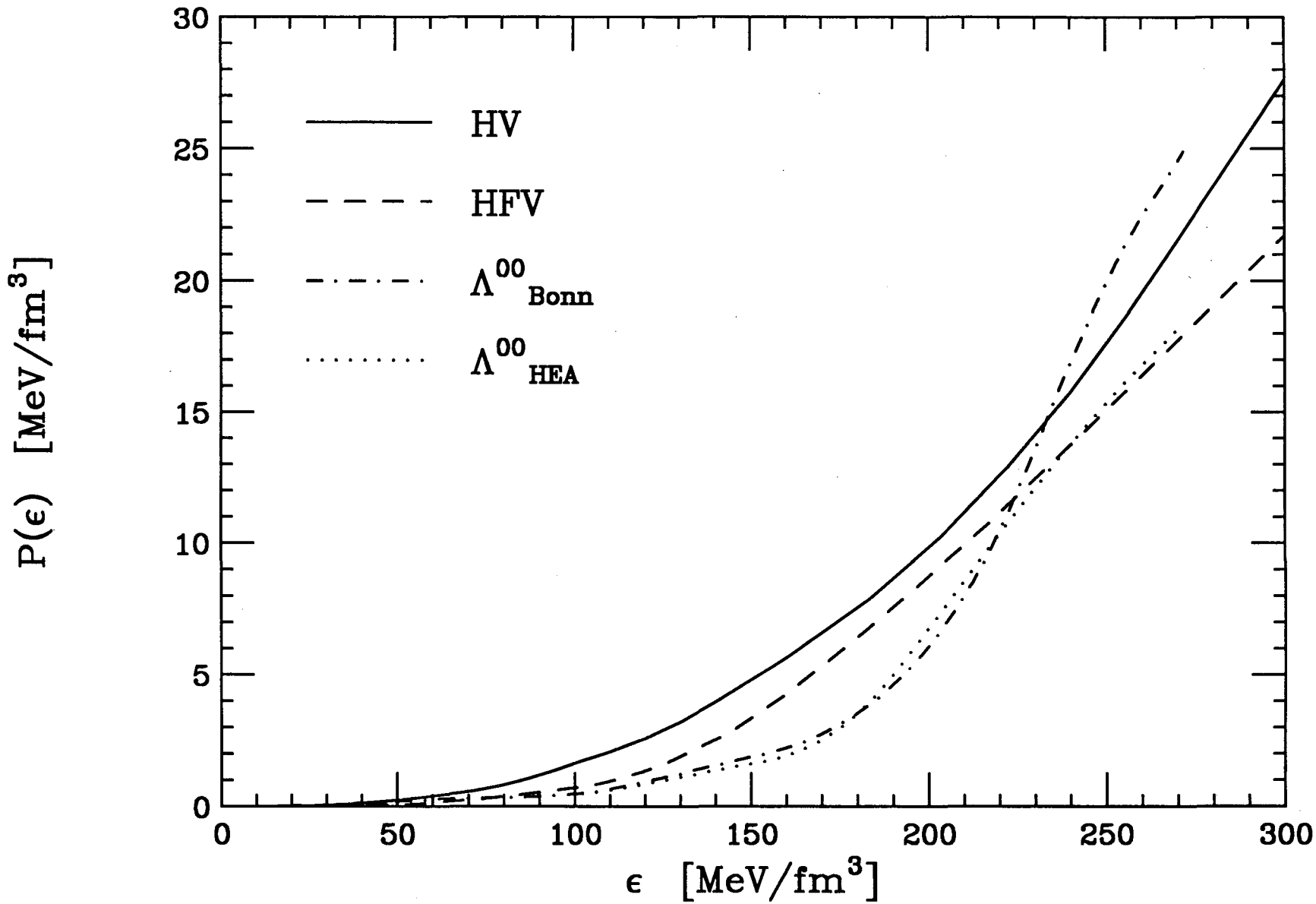
HV
HFV
Λ^{00}_{Bonn}
Λ^{00}_{HEA}
P(ϵ) [MeV/fm^3]
ϵ [MeV/fm^3]
0
5
10
15
20
25
30
0
50
100
150
200
250
300

Figure 1

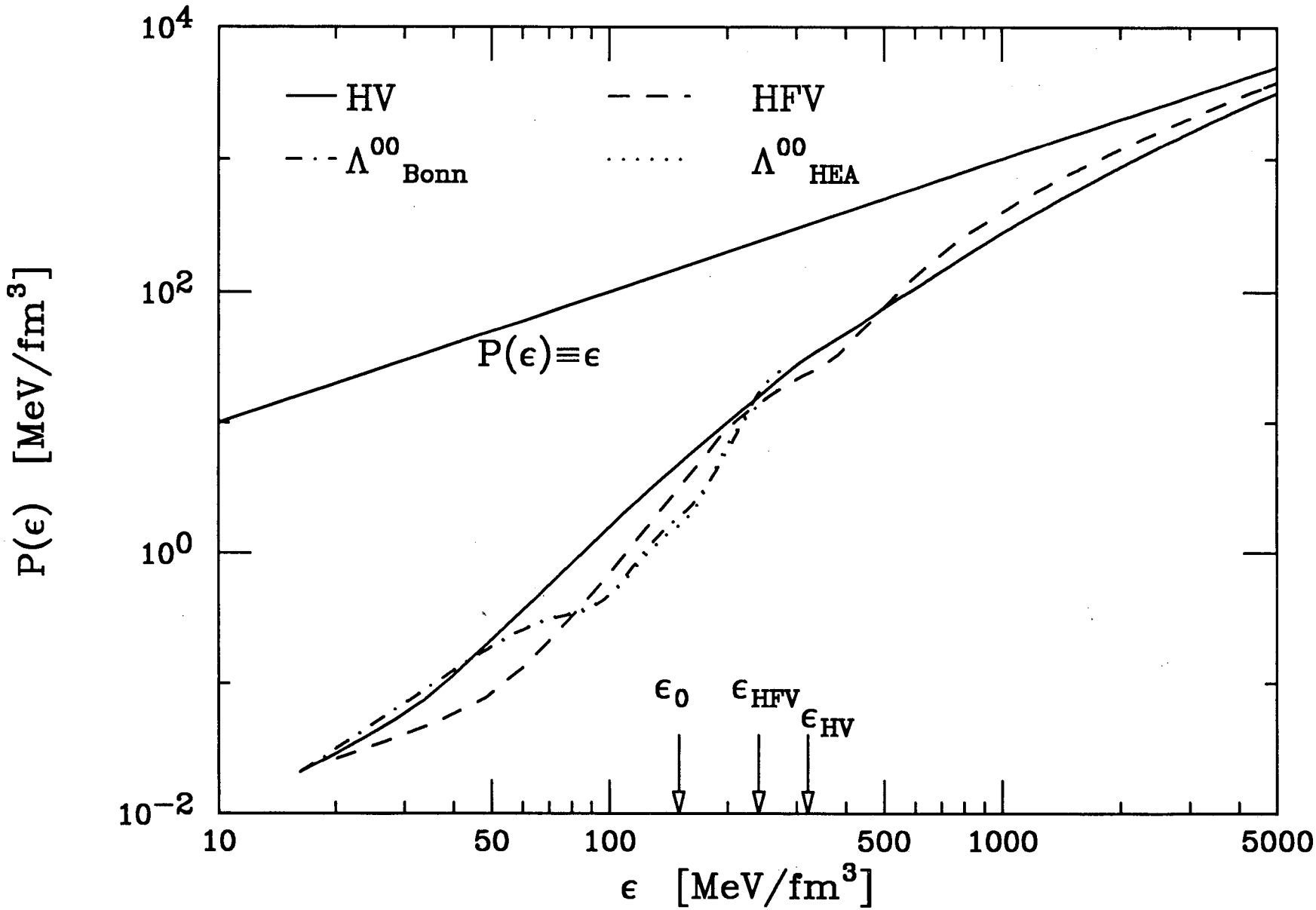
HV
HFV
Λ^{00}_{Bonn}
Λ^{00}_{HEA}
$P(\epsilon)\equiv\epsilon$
ϵ_0
ϵ_{HFV}
ϵ_{HV}
10^4
10^2
10^0
10^{-2}
10
50
100
500
1000
5000
$P(\epsilon)$ [MeV/fm^3]
ϵ [MeV/fm^3]

Figure 2

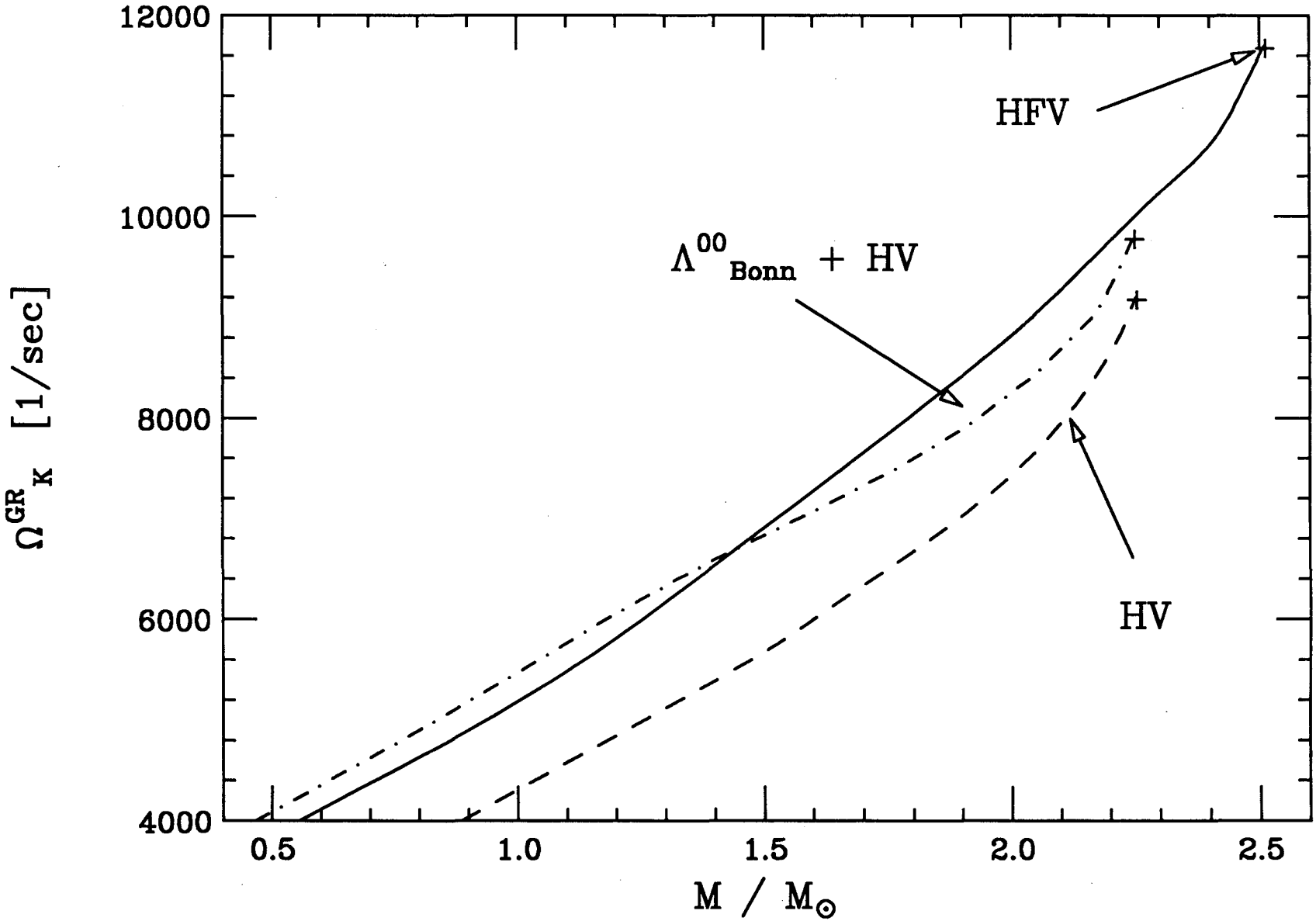
12000
10000
8000
6000
4000
0.5
1.0
1.5
2.0
2.5
Ω^{GR}_K [1/sec]
M / $M_\odot$
HFV
Λ^{00}_{Bonn} + HV
HV

Figure 3

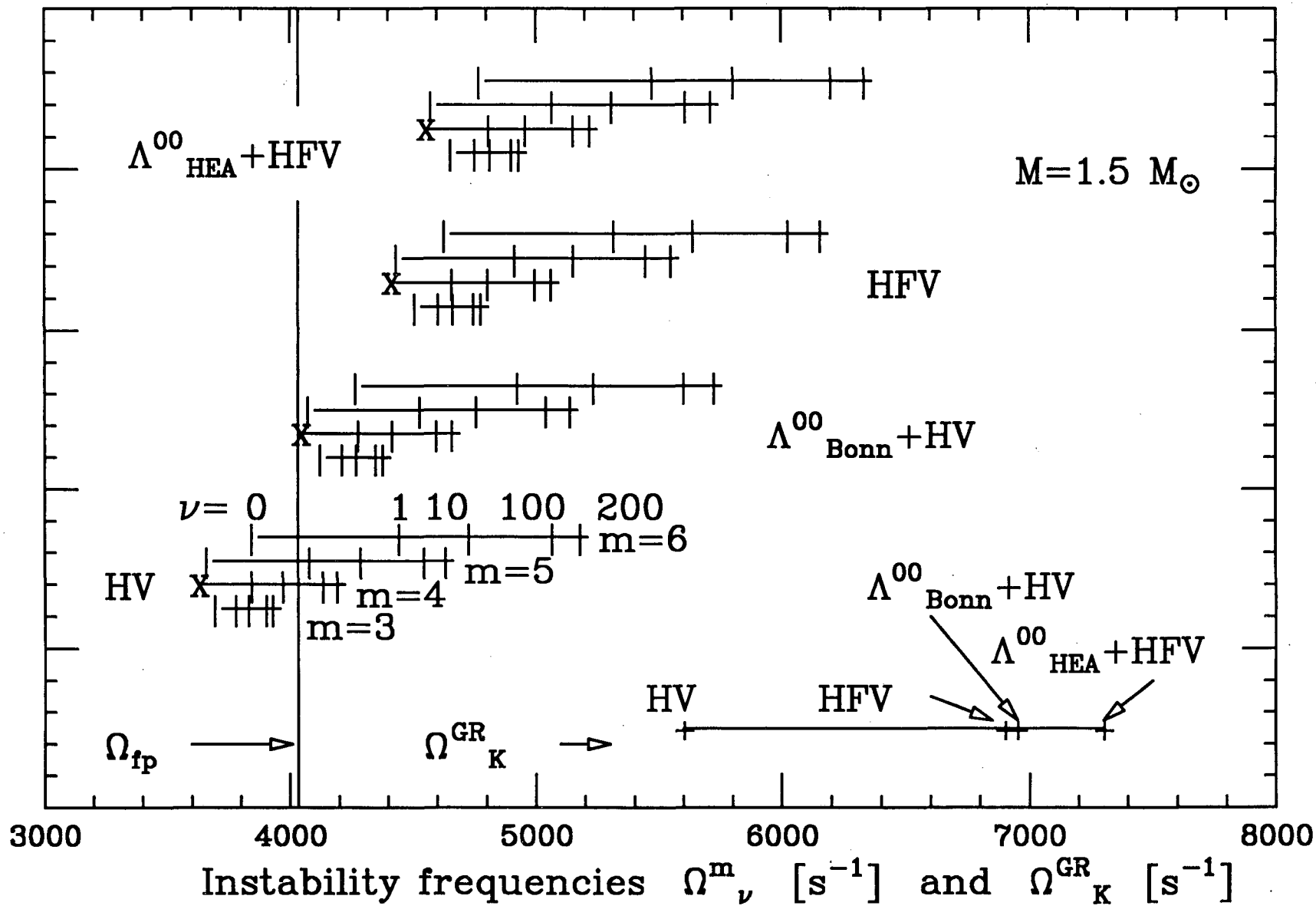
Λ^{00}_{HEA}+HFV
M=1.5 $M_\odot$
HFV
Λ^{00}_{Bonn}+HV
ν= 0
1 10 100 200
m=6
m=5
m=4
m=3
HV
Λ^{00}_{Bonn}+HV
Λ^{00}_{HEA}+HFV
HV
HFV
Ω_{fp}
Ω^{GR}_{K}
3000
4000
5000
6000
7000
8000
Instability frequencies Ω^{m}_{ν} [s^{-1}] and Ω^{GR}_{K} [s^{-1}]

Figure 4

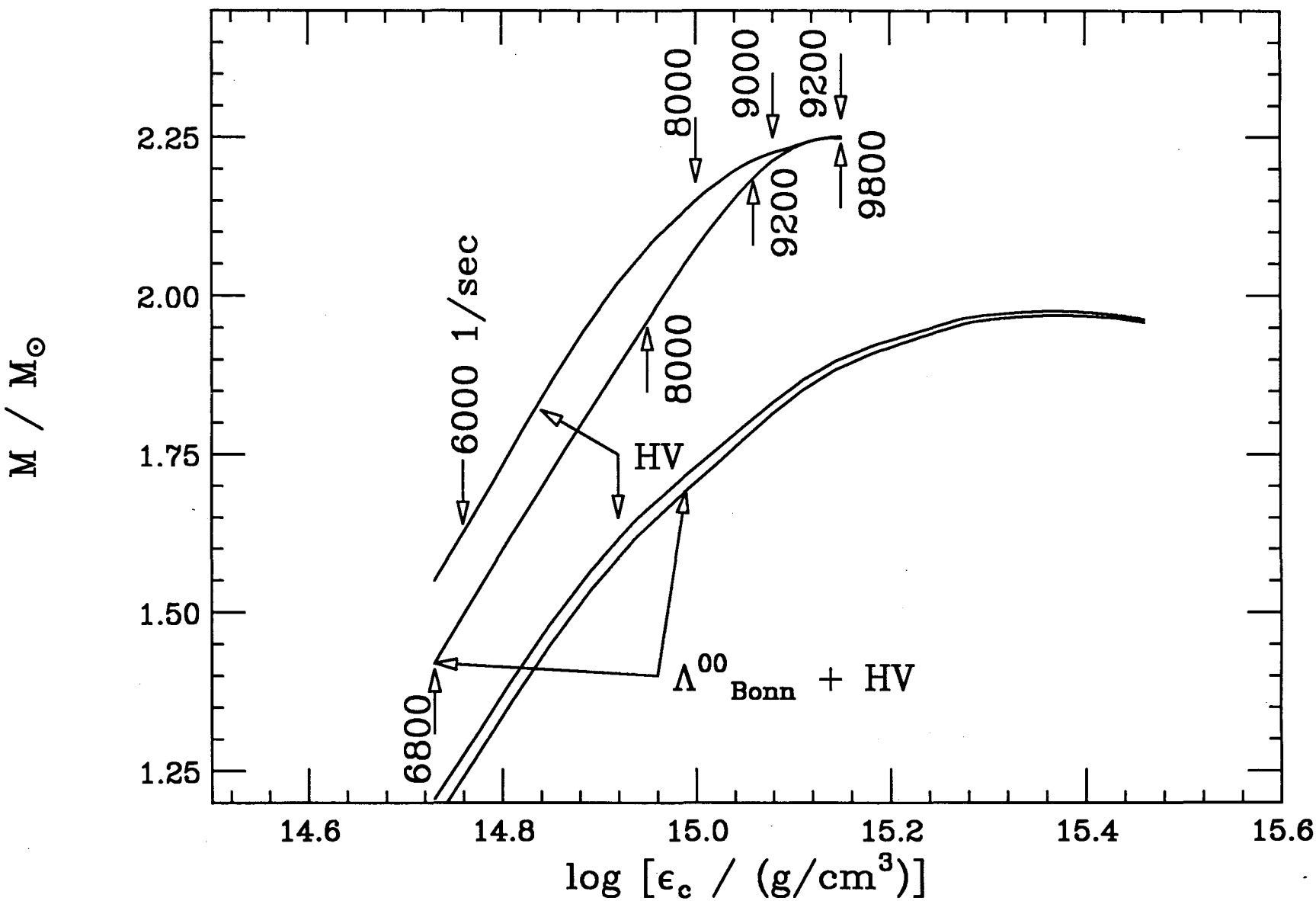
2.25
2.00
1.75
1.50
1.25
M / M⊙
14.6
14.8
15.0
15.2
15.4
15.6
log [ϵc / (g/cm3)]
6000 1/sec
8000
9000
9200
9800
9200
8000
6800
HV
Λ00Bonn + HV

Figure 5

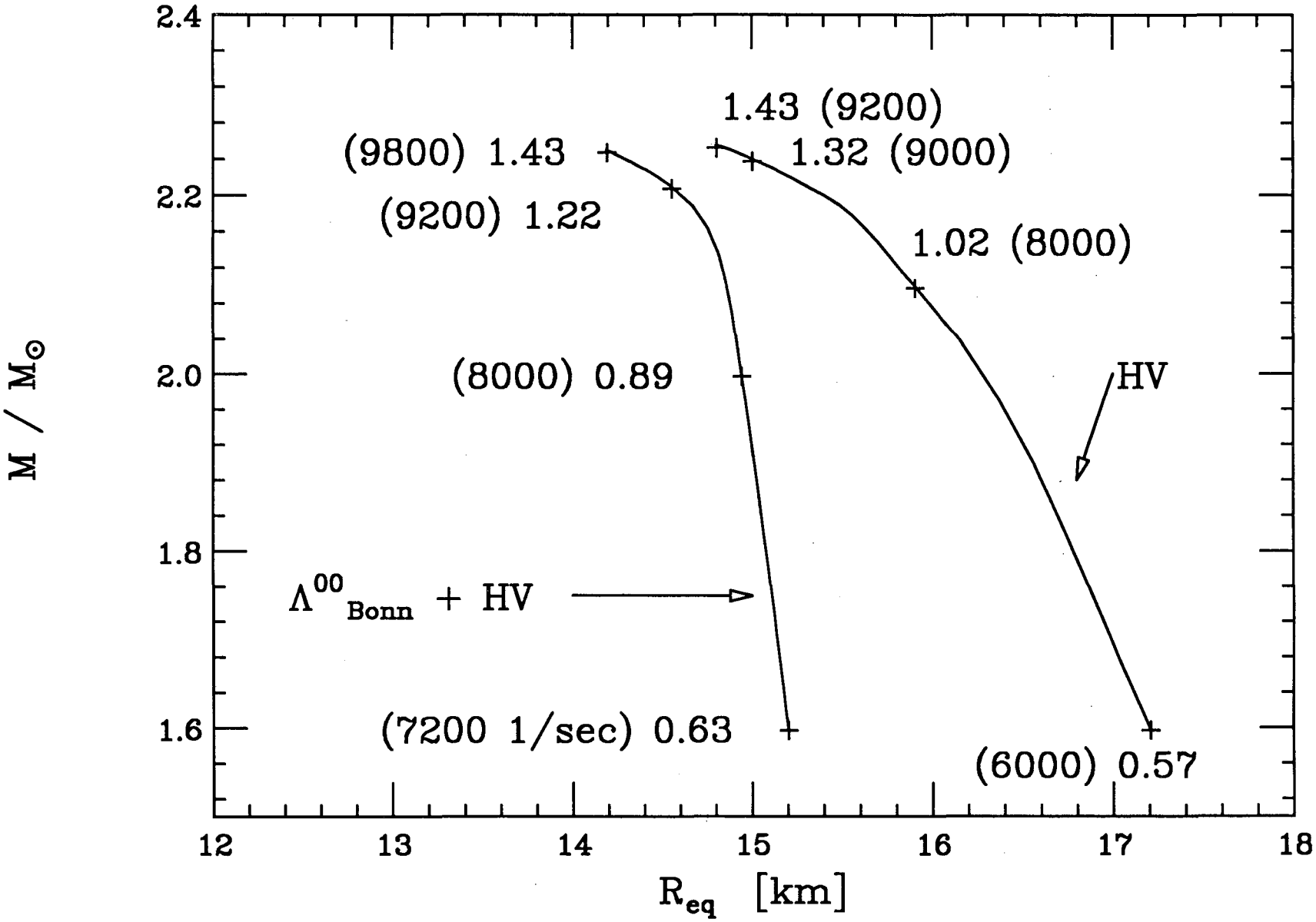
2.4
2.2
2.0
1.8
1.6
12
13
14
15
16
17
18
M / M⊙
R_eq [km]
1.43 (9200)
1.32 (9000)
(9800) 1.43
(9200) 1.22
1.02 (8000)
(8000) 0.89
HV
Λ^00_Bonn + HV
(7200 1/sec) 0.63
(6000) 0.57

Figure 6

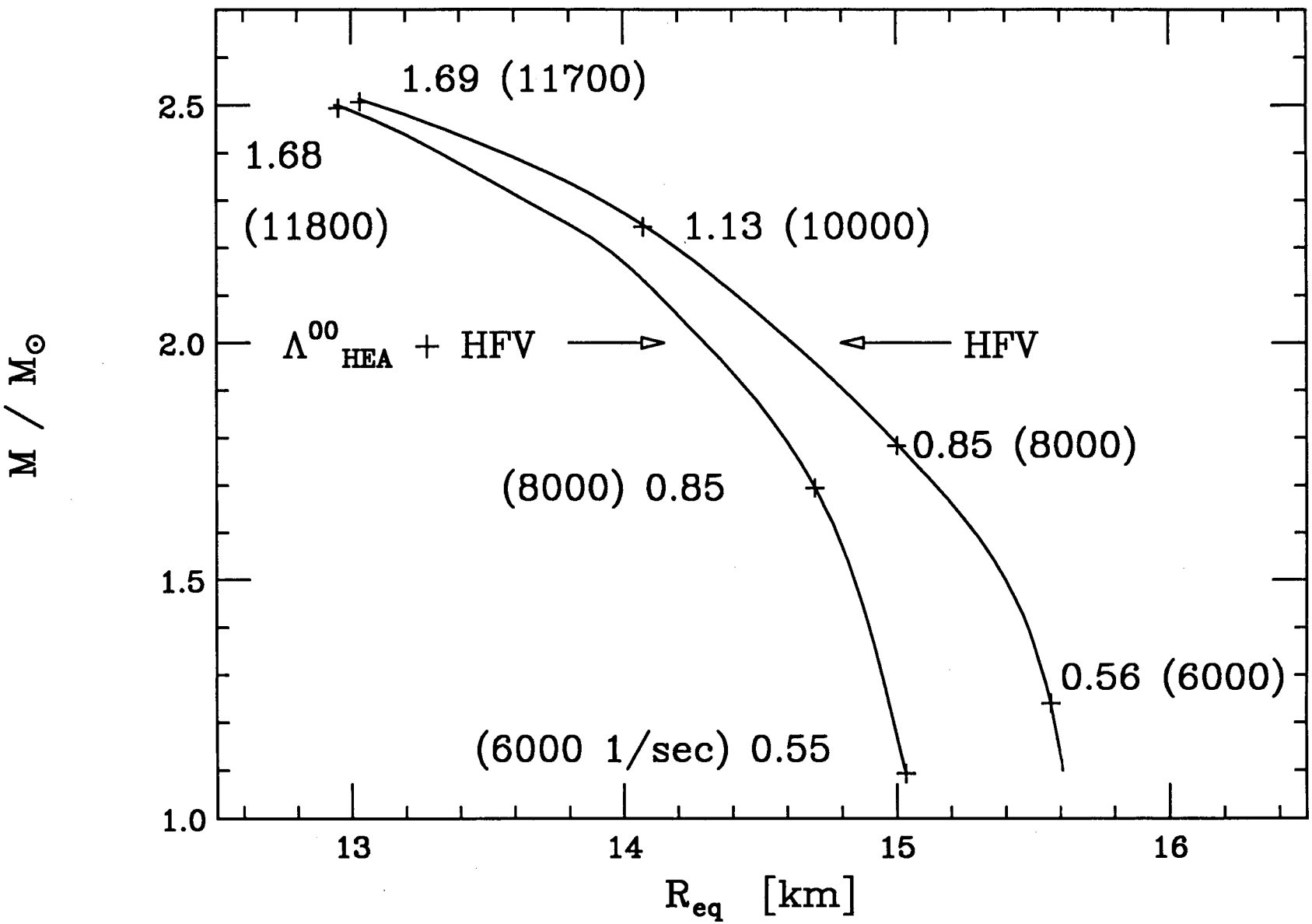
1.69 (11700)
1.68
(11800)
1.13 (10000)
Λ^{00}_{HEA} + HFV
HFV
0.85 (8000)
(8000) 0.85
0.56 (6000)
(6000 1/sec) 0.55
2.5
2.0
1.5
1.0
13
14
15
16
$M / M_\odot$
R_{eq} [km]

Figure 7

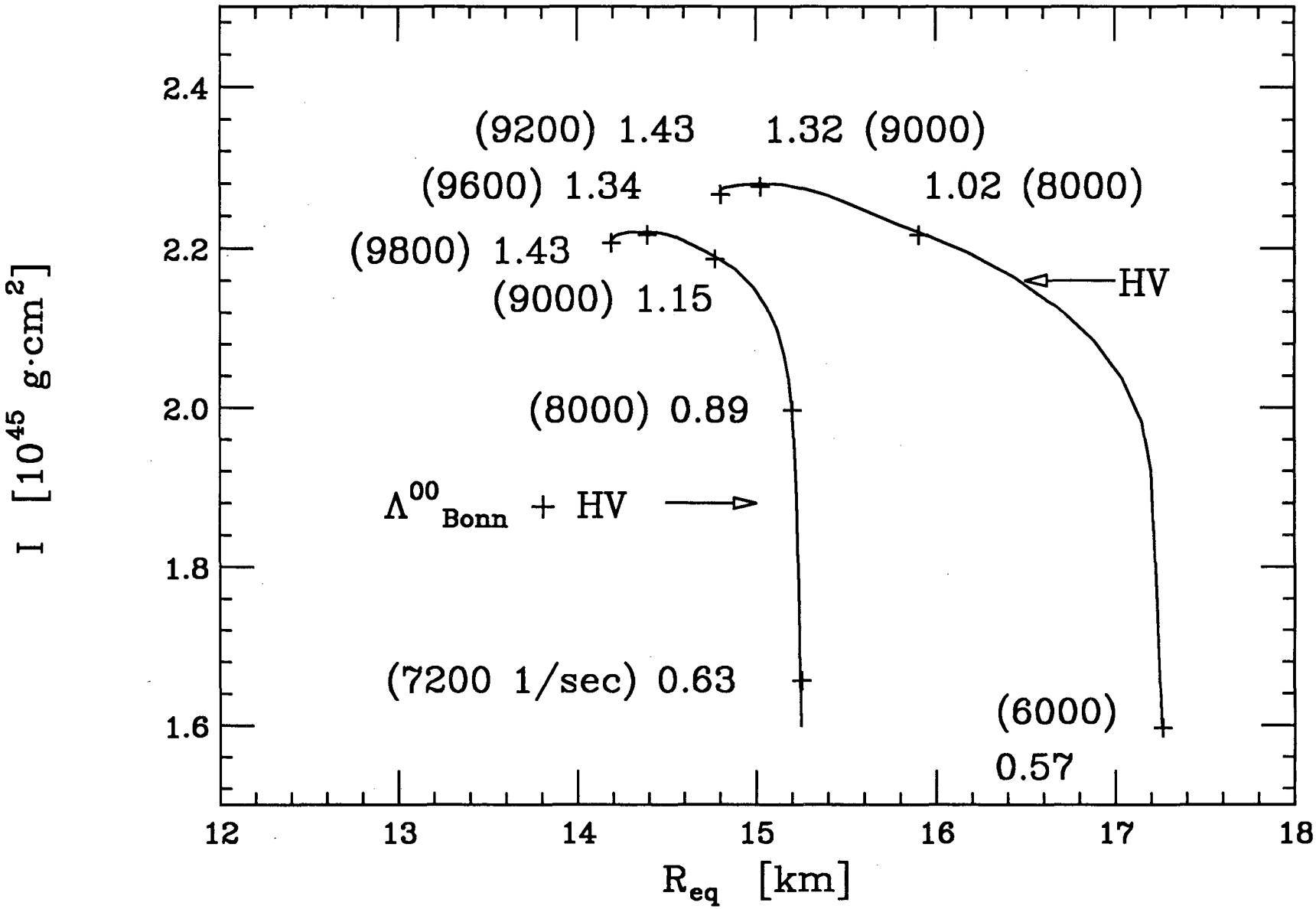
(9200) 1.43
1.32 (9000)
(9600) 1.34
1.02 (8000)
(9800) 1.43
(9000) 1.15
HV
(8000) 0.89
Λ^{00}_{Bonn} + HV
(7200 1/sec) 0.63
(6000)
0.57
2.4
2.2
2.0
1.8
1.6
12
13
14
15
16
17
18
I [10^{45} g·cm^2]
R_{eq} [km]

Figure 8

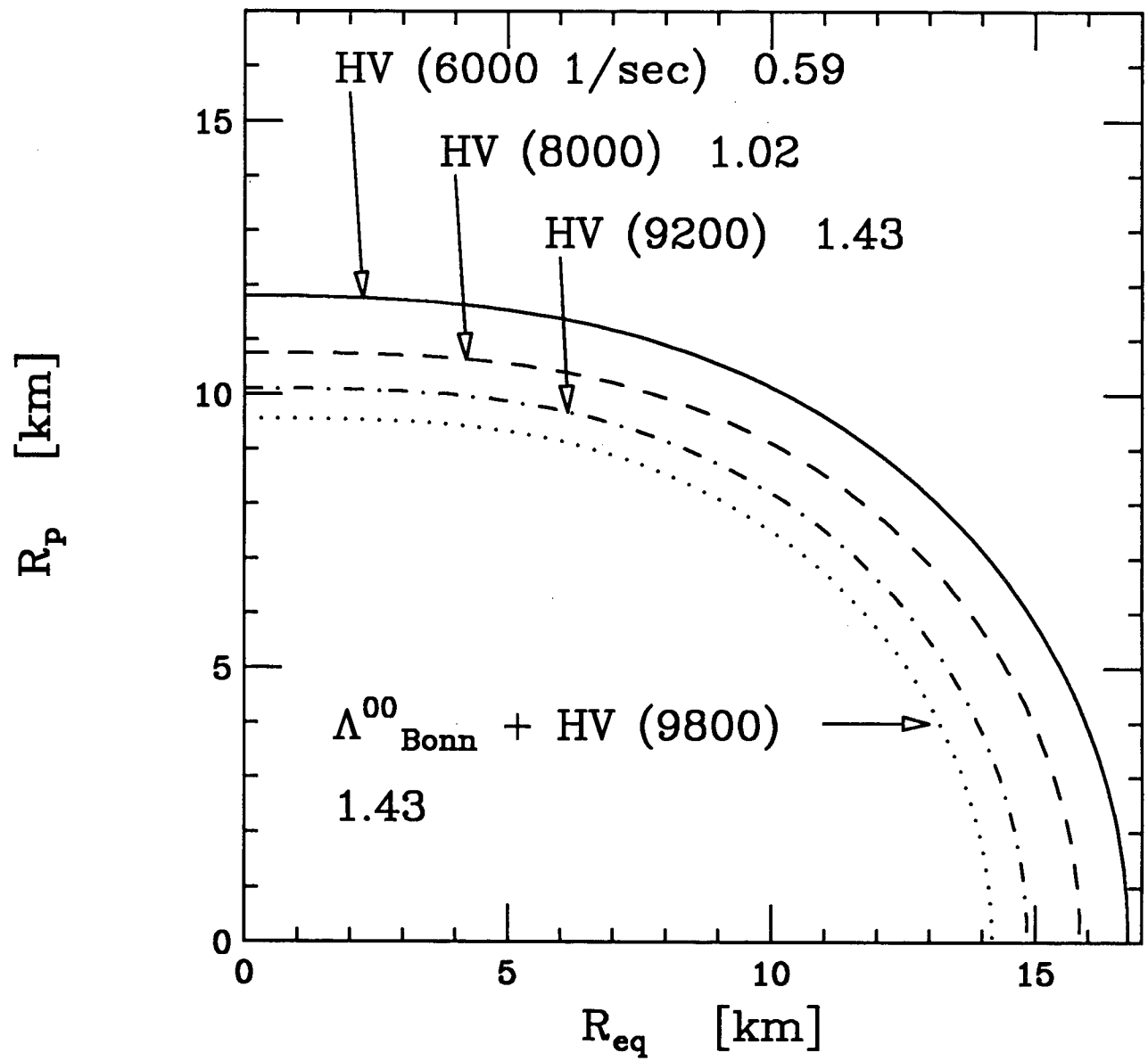
HV (6000 1/sec) 0.59
HV (8000) 1.02
HV (9200) 1.43
Λ^{00}_{Bonn} + HV (9800)
1.43
R_p [km]
R_{eq} [km]
0
5
10
15

Figure 9

LAWRENCE BERKELEY LABORATORY
UNIVERSITY OF CALIFORNIA
INFORMATION RESOURCES DEPARTMENT
BERKELEY, CALIFORNIA 94720